DTIC FILE COPY

AD-A226 070

REPORT DOCUMENTATION PAGE

Form Approved
OMB No. 0704-0188

1. AGENCY USE ONLY *(Leave blank)*

2. REPORT DATE

3. REPORT TYPE AND DATES COVERED
Final Report/1 Aug 86-30 Nov 89

4. TITLE AND SUBTITLE
Compact Millimeter-Wave Devices: Cherenkov CARM, Voltage CARM and High Harmonic Gyrotron

5. FUNDING NUMBERS
61102F/2301/A8

6. AUTHOR(S)
Neville C. Luhmann, Jr.

7. PERFORMING ORGANIZATION NAME(S) AND ADDRESS(ES)
University of California
Electrical Engineering Department
Los Angeles, CA 90024

8. PERFORMING ORGANIZATION REPORT NUMBER
AFOSR-TR- 90 0880

9. SPONSORING/MONITORING AGENCY NAME(S) AND ADDRESS(ES)
AFOSR/NP
Bolling AFB DC 20332-6448

10. SPONSORING/MONITORING AGENCY REPORT NUMBER
AFOSR-86-0199

11. SUPPLEMENTARY NOTES

12a. DISTRIBUTION/AVAILABILITY STATEMENT
Approved for public release; distribution is unlimited.

12b. DISTRIBUTION CODE

13. ABSTRACT *(Maximum 200 words)*
The dielectric-loaded CARM experiments were extremely dissappointing. Even with a high quality electron beam, the performance of the device did not improve. The analytical theory of Bragg reflectors was developed. The reflection is found by solving the coupled differential equations by the eigenvalue/eiginvector method.

14. SUBJECT TERMS
eigenvalue/eiginvector, dielectric-loaded CARM

15. NUMBER OF PAGES

16. PRICE CODE

17. SECURITY CLASSIFICATION OF REPORT	18. SECURITY CLASSIFICATION OF THIS PAGE	19. SECURITY CLASSIFICATION OF ABSTRACT	20. LIMITATION OF ABSTRACT
UNCLASSIFIED	UNCLASSIFIED	UNCLASSIFIED	SAR

90 088

NSN 7540-01-280-5500

Standard Form 298 (Rev. 2-89)
Prescribed by ANSI Std. Z39-18

GENERAL INSTRUCTIONS FOR COMPLETING SF 298

The Report Documentation Page (RDP) is used in announcing and cataloging reports. It is important that this information be consistent with the rest of the report, particularly the cover and title page. Instructions for filling in each block of the form follow. It is important to ***stay within the lines*** to meet ***optical scanning requirements***.

Block 1. Agency Use Only *(Leave blank)*.

Block 2. Report Date. Full publication date including day, month, and year, if available (e.g. 1 Jan 88). Must cite at least the year.

Block 3. Type of Report and Dates Covered. State whether report is interim, final, etc. If applicable, enter inclusive report dates (e.g. 10 Jun 87 - 30 Jun 88).

Block 4. Title and Subtitle. A title is taken from the part of the report that provides the most meaningful and complete information. When a report is prepared in more than one volume, repeat the primary title, add volume number, and include subtitle for the specific volume. On classified documents enter the title classification in parentheses.

Block 5. Funding Numbers. To include contract and grant numbers; may include program element number(s), project number(s), task number(s), and work unit number(s). Use the following labels:

C	Contract	PR	Project
G	Grant	TA	Task
PE	Program Element	WU	Work Unit Accession No.

Block 6. Author(s). Name(s) of person(s) responsible for writing the report, performing the research, or credited with the content of the report. If editor or compiler, this should follow the name(s).

Block 7. Performing Organization Name(s) and Address(es). Self-explanatory.

Block 8. Performing Organization Report Number. Enter the unique alphanumeric report number(s) assigned by the organization performing the report.

Block 9. Sponsoring/Monitoring Agency Name(s) and Address(es). Self-explanatory.

Block 10. Sponsoring/Monitoring Agency Report Number. *(If known)*

Block 11. Supplementary Notes. Enter information not included elsewhere such as: Prepared in cooperation with...; Trans. of...; To be published in.... When a report is revised, include a statement whether the new report supersedes or supplements the older report.

Block 12a. Distribution/Availability Statement. Denotes public availability or limitations. Cite any availability to the public. Enter additional limitations or special markings in all capitals (e.g. NOFORN, REL, ITAR).

- DOD - See DoDD 5230.24, "Distribution Statements on Technical Documents."
- DOE - See authorities.
- NASA - See Handbook NHB 2200.2.
- NTIS - Leave blank.

Block 12b. Distribution Code.

- DOD - Leave blank.
- DOE - Enter DOE distribution categories from the Standard Distribution for Unclassified Scientific and Technical Reports.
- NASA - Leave blank.
- NTIS - Leave blank.

Block 13. Abstract. *Include a brief (Maximum 200 words)* factual summary of the most significant information contained in the report.

Block 14. Subject Terms. Keywords or phrases identifying major subjects in the report.

Block 15. Number of Pages. Enter the total number of pages.

Block 16. Price Code. Enter appropriate price code *(NTIS only)*.

Blocks 17. - 19. Security Classifications. Self-explanatory. Enter U.S. Security Classification in accordance with U.S. Security Regulations (i.e., UNCLASSIFIED). If form contains classified information, stamp classification on the top and bottom of the page.

Block 20. Limitation of Abstract. This block must be completed to assign a limitation to the abstract. Enter either UL (unlimited) or SAR (same as report). An entry in this block is necessary if the abstract is to be limited. If blank, the abstract is assumed to be unlimited.

FINAL REPORT

AFOSR-86-0199

COMPACT MILLIMETER-WAVE DEVICES: CHERENKOV CARM, HIGH VOLTAGE CARM AND HIGH HARMONIC GYROTRON

1 AUGUST 1986 - 30 NOVEMBER 1989

Neville C. Luhmann, Jr.

University of California

Electrical Engineering Department

Los Angeles, CA 90024

A-1

APPROACH

During the last contract period, three interactions for mm-wave generation were under investigation. In the prebunched, high harmonic gyrotron, rf-accelerated axis-encircling electrons are in synchronism with a high order azimuthal TE_{n1} mode with $\omega_{out} = n\Omega_c + k_{\|}v_{\|}$, thereby reducing the requisite magnetic field of a gyrotron by n (n $\approx$ 2 - 30). Also, the ability of the gyroresonant rf accelerator to produce an azimuthally bunched, helical beam is exploited by setting $\omega_{acc} = \omega_{out}/n$, so that all electrons enter the gyrotron cavity at the optimal rf phase. In this first order interaction, all electrons lose energy to the wave, thereby greatly increasing the efficiency as well as reducing mode competition problems.

In the cyclotron autoresonance maser, gyrating electrons remain in gyroresonance with a copropagating wave with $v_{ph} = c$, even as they lose energy to the wave, thereby yielding high efficiency. A CARM can generate extremely high power due to reduced attenuation of the rf due to its propagation far above cutoff. Also, compared to a gyrotron, a CARM requires lower magnetic field due to a large Doppler frequency upshift.

Another interaction being studied is the Dielectric Loaded CARM, where the previously described highly efficient cyclotron autoresonant interaction, which is predicted to occur for $v_{ph} = c$, is accessed by employing a dielectric lined waveguide to slow the phase velocity of the electromagnetic wave, so that a much lower electron beam voltage can be employed.

We are also developing a frequency selective cavity to operate these interactions as oscillators. In a Bragg resonator, the two reflectors merely consist of corrugated waveguide. A wave which satisfies the Bragg condition, $\lambda_{\|} = 2\ell$, where $\lambda_{\|}$ is the axial wavelength and ℓ is the corrugation period, is reflected through the principle of destructive interference.

PROGRESS (Jan. 1, 1989 - Dec. 31, 1989)

I. Prebunched High Harmonic Gyrotron

To compare with the prebunched cavity, which had yielded an unprecedented conversion power of 6.7 kW at the third harmonic, we built and tested two non-prebunched gyrotron cavities, one a control experiment (roughly same dimensions) and the other a more optimized gyrotron. Both cavities yielded an order of magnitude less power than the prebunched cavity, showing that the prebunched gyrotron is an important interaction. The experimental results were described along with the analytical theory in the manuscript, "Prebunched High-Harmonic Gyrotron," by C.S. Kou, D.B. McDermott, N.C. Luhmann, Jr. and K.R. Chu, which was sent to the IEEE Trans. on Plasma Science's Special Issue on High-Power Microwave Generation (subsequently published - IEEE Trans. on Plasma Science 18, 343 (1990)).

II. Dielectric Loaded CARM

The focus of our efforts was to improve the quality of the electron beam. To reduce the axial velocity spread, a new gyroresonant wiggler was fabricated with a period twice as long as the initial one, which should reduce the velocity spread due to the transverse pump inhomogeneity by a factor of four. The transverse velocity of the electron beam transformed by this wiggler was measured and very favorably compared to simulation results. Despite these and other modifications, the performance of the device did not improve. We were limited to a maximum $k_{||}c/\omega$ of 0.7.

III. High Voltage CARM

We entered into a collaboration with Drs. Caplan and Kulke of LLNL on a 400 MW, 250 GHz CARM driven by an induction linac. We have supplied the superconducting solenoid for the project and will perform measurements of the rf output. Using the CARM simulation code which Dr. Caplan supplied us, we have designed and optimized many high power CARMs for various applications. A 150 MW, 17 GHz CARM driven by a 1 MV, 400 A electron beam with 40% efficiency was designed to satisfy DOD's super power microwave needs as well as DOE's future driver requirements for high gradient linacs.

The construction of a CARM proof of principle experiment has progressed. A 60 ft^3 oil tank for the 800 kV 20:1/40:1 dual step-up transformer has been assembled and mounted on a rail system. The experiment will be performed at 10 GHz in our 2 m long, 3 kG solenoid with an expected output power of 20 MW.

IV. Bragg Reflectors

The analytical theory of Bragg reflectors was developed. The reflection is found by solving the coupled differential equations by the eigenvalue/ eigenvector method.

Bragg reflectors with rectangular corrugation have been electroformed and measured. The reflection from the rectangular corrugations was found to be as high as 98-99% for a certain narrow range of frequency. The data agrees with analytical theory fairly well, except that the coupling was much larger than expected from Fourier decomposition. The pure $TE_{11} - TE_{11}$ coupling resonance was observed as well as the $TE_{11} - TM_{11}$ intercoupling resonance.

PUBLICATIONS AND PRESENTATIONS (Jan. 1, 1989 - Dec. 31, 1989)

"Prebunched High Harmonic Gyrotron," by C.S. Kou, D.B. McDermott and N.C. Luhmann, Jr., submitted to IEEE Trans Plasma Science Special Issue on High Power Microwave Generation, (subsequently published in Vol. 18, p. 343 (1990)).

H.B. Cao, D.B. McDermott and N.C. Luhmann, Jr., "Initial Operation of a Cherenkov CARM," Proceedings of 1989 SPIE Conf. on Microwave and Particle Beams 1061, pp. 248-253, Los Angeles, California, 1989.

Q.S. Wang, A.T. Lin, N.C. Luhmann, Jr., D.B. McDermott and K.R. Chu, "Cyclotron Autoresonance Maser (CARM) EC Heating Source for High Field Tokamaks," Proceedings of 1989 SPIE Conf. on Microwave and Particle Beams 1061, pp. 254-261, Los Angeles, California, 1989.

C.S. Kou, D.B. McDermott and N.C. Luhmann, Jr., "Prebunched High Harmonic Gyrotron," Proceedings of 1989 SPIE Conf. on Microwave and Particle Beams 1061, pp. 262-268, Los Angeles, California, 1989.

"Dielectric Loaded CARM," K.C. Leou, D.B. McDermott and N.C. Luhmann, Jr., Bull. Am. Phys. Soc. 34, 2088 (1989).

"High Power CARM," Q.S. Wang, A.T. Lin, N.C. Luhmann, Jr., D.B. McDermott and K.R. Chu, Bull. Am. Phys. Soc. 34, 2089 (1989).

"Design of a Bragg Resonator," C.K. Chong, D.B. McDermott, M. Razeghi, and N.C. Luhmann, Jr., Bull. Am. Phys. Soc. 34, 2092 (1989).

"Prebunched High Harmonic Gyrotron," C.S. Kou, D.B. McDermott and N.C. Luhmann, Jr., Bull Am. Phys. Soc. 34, 2092 (1989).

"Bragg Resonator for Selective Feedback in Overmoded Oscillators," C.K. Chong, M.M. Razeghi, D.B. McDermott and N.C. Luhmann, Jr., Fourteenth Int. Conf. IR & mm-Waves, Wurzburg, Germany, 1989.

"High Power CARM," Q.S. Wang, A.T. Lin, N.C. Luhmann, Jr., D.B. McDermott and K.R. Chu, Fourteenth Int. Conf. IR & mm-Waves, Wurzburg, Germany, 1989.

"Dielectric Loaded CARM," K.C. Leou, D.B. McDermott and N.C. Luhmann, Jr., Fourteenth Int. Conf. IR & mm-Waves, Wurzburg, Germany, 1989.

"Prebunched High Harmonic Gyrotron," C.S. Kou, D.B. McDermott and N.C. Luhmann, Jr., Digest of Fourteenth Int. Conf. IR & mm-Waves, Wurzburg, Germany, 1989.

"Cyclotron Autoresonance Maser Amplifiers and Oscillators," Q.S. Wang, C.S. Kou, K.C. Leon, C.K. Chong, D.B. McDermott, A.T. Lin, N.C. Luhmann, Jr., M. Caplan, B. Kulke, A. Salop and K.R. Chu, Digest International Electron Device Meeting, p. 759, Washington, D.C., 1989.

"Bragg Resonator for Selective Feedback in Overmoded Oscillators," C.K. Chong, M.M. Razeghi, D.B. McDermott, N.C. Luhmann, Jr., M. Caplan, and B. Kulke, Submitted to

1990 SPIE Conf. on High Power Microwaves and Particle Beams (Subsequently published in Digest of 1990 SPIE Conf. on High Power Microwaves and Particle Beams 1226, p. 228, (1990)).

"High Power CARM for High Gradient RF Linac," Q.S. Wang, D.B. McDermott, A.T. Lin, N.C. Luhmann, Jr. and K.R. Chu, Submitted to 1990 SPIE Conf. on High Power Microwaves and Particle Beams (Subsequently published in Digest of 1990 SPIE Conf. on High Power Microwaves and Particle Beams 1226, p 220, Los Angeles, California, 1990).

PROGRESS (Aug. 1, 1987 - July 31, 1988):

I. Prebunched High Harmonic Gyrotron

The analytic theory of the prebunched harmonic gyrotron has been developed including the electron beam's axial velocity spread and guiding center spread. The derivation yields the expected output power as a function of beam current. An experiment has been performed at the third harmonic of the cyclotron frequency. Two output cavities were used - one satisfied the prebunching condition and the other was mistuned by 2%. The prebunched cavity generated a power of 125 kW/A^2 in the linear regime and a peak power of 6.7 kW in very good agreement with theory, whereas the non-prebunched cavity yielded approximately two orders of magnitude less power. The predicted dependence of the prebunched gyrotron's output power on the square of the beam current has been verified. The start of oscillation current is effectively zero.

II. Cyclotron Autoresonance Maser

We have benefited from the collaboration of Drs. K.R. Chu and A.T. Lin. They have found the stability conditions for the CARM amplifier. It is bounded by the gyro-TWT at low magnetic field and absolute instability at high magnetic field. Dr. Chu has derived the magnetic field tuning range and the resulting frequency upshift and growth rate for a 700 kV CARM operated in either the TE_{11} or TE_{01} mode of cylindrical guide. Dr. Lin has performed numerical simulation of CARMs appropriate for a) EC heating of fusion plasmas and b) high power (1 kJ/μs) microwave weapons.

An experiment is being assembled to test the CARM's stability and features of efficiency enhancement and frequency upshift. The components for a 25 kV, 2 Ω, 10 Hz, 2 μsec pulse modulator have been received. An 800 kV, 20:1/40:1 dual step-up transformer and a 400 kV SLAC electron gun have also been received. A 60 kG superconducting solenoid with an extra uniform region for gyroresonant velocity transformation has been ordered. The proof of principle experiment will be performed at 33 GHz with an expected output power of 10 MW including the deleterious effect of a 1% axial velocity spread and a 52% guiding center spread, as predicted by Dr. Lin's simulations.

III. Cherenkov Cyclotron Autoresonance Maser

Velocity transformation in an improved gyroresonant wiggler has been measured. A thin pencil electron beam passed through a small aperture before propagating through the wiggler on its way toward a Uranium glass scintillation plate. The fluorescent image of the resultant electron ring yielded a direct measurement of the electron's Larmor radius from which the transverse velocity can be deduced since the magnetic field is known. The dependence of the final $v_\perp$ on the background axial magnetic field and the wiggler's transverse magnetic field has been compared to simulation results. Agreement is very good.

The helical electron beam was then guided through the Cherenkov CARM. No radiation was generated in the first experiment. A serious problem with the system was that the magnetic fields for the CARM and wiggler regions could not be independently varied. The two solenoids were energized by the same power supply. We are currently reconfiguring the magnetic system so that a separate power supply will energize each solenoid. The Cherenkov CARM will then be retested.

Before settling on the gyroresonant wiggler to transform the input pencil electron beam into the desired helical beam, we tested a magnetic kicker. The electron beam was passed through an iron ring within the magnetic field. The ring produces a non-adiabatic depression in the field. The v_zB_r azimuthal force produces the needed transverse velocity. Unfortunately, we expect that the α of the electron beam is a strong function of radius since B_r is a first order modified Bessel function. Yet, this configuration has produced a beam with a quality good enough to excite a gyrotron cavity. The transformed 500 kW beam was directed through a gyrotron cavity (no dielectric) with a radius and length of 0.871 cm and 8.712 cm, respectively. Approximately 20 kW has been emitted at 10.5 GHz form the cavity's TE_{11} mode. The measured start of oscillation current suggests that the α of the beam was roughly 0.9. Of much interest, monochromatic second harmonic emission occurs at the 1 kW power level at 16.9 Ghz, which corresponds to the TE_{21} mode. Second harmonic emission is predicted to peak for electrons on axis for the TE_{21} mode. Similarly, the third harmonic should peak for electrons on axis for the TE_{31} mode.

AFOSR PROGRAM MANAGER: Dr.RobertBarker

Publications and Presentations (Aug. 1, 1987 - July 31, 1988):

"A Cherenkov Cyclotron Autoresonance Maser," D.B. McDermott, Haibo Cao and N.C. Luhmann, Jr., *Int. J. Electronics*, 65, 477 (1988).

"Prebunched High Harmonic Gyrotron," C.S. Kou, D.B. McDermott and N.C. Luhmann, Jr., *Bull. Am. Phys. Soc.*, 32, 1864 (1987).

"Cyclotron Autoresonant Maser (CARM) Heating Source for High Field Tokamaks," N.C. Luhmann, Jr., A.T. Lin, and D.B. McDermott. *Bull. Am. Phys. Soc.*, 32, 1865, (1987).

"A Cherenkov CARM," *Bull. Am. Phys. Soc.*, 32, 1865 (1987).

"Cyclotron Autoresonance Maser (CARM) EC Heating Source for High Field Tokamaks," A.T. Lin, N.C. Luhmann, Jr., D.B. McDermott and K.R. Chu, Invited Paper, *Digest of Twelfth Int. Conf. IR & mm-Waves*, Orlando, Florida, 1987.

"Initial Operation of a Cherenkov Autoresonance Maser," H. Cao, D.B. McDermott and N.C. Luhmann, Jr., 1988 IEEE Int. Conf. Plasma Science, Seattle, Washington, 1988.

"Operation of a Prebunched High Harmonic Cyclotron," C.S. Kou, K.J. Knudsen, D.B. McDermott and N.C. Luhmann, Jr., 1988 IEEE Int. Conf. Plasma Science, Seattle, Washington.

PROGRESS (Aug. 1, 1987 - Dec. 31, 1988):

I. Prebunched High Harmonic Gyrotron

The analytic theory of the prebunched harmonic gyrotron has been developed including the electron beam's axial velocity spread and guiding center spread. The derivation yields the expected output power as a function of beam current. An experiment has been performed at the third harmonic of the cyclotron frequency. Two output cavities were used - one satisfied the prebunching condition and the other was mistuned by 2%. The prebunched cavity generated a power of 125 kW/A^2 in the linear regime and a peak power of 6.7 kW in very good agreement with theory, whereas the non-prebunched cavity yielded approximately two orders of magnitude less power. The predicted dependence of the prebunched gyrotron's output power on the square of the beam current has been verified. The start of oscillation current is effectively zero.

II. Cyclotron Autoresonance Maser

We have benefited from the collaboration of Drs. K.R. Chu and A.T. Lin. They have found the stability conditions for the CARM amplifier. It is bounded by the gyro-TWT at low magnetic field and absolute instability at high magnetic field. Dr. Chu has derived the magnetic field tuning range and the resulting frequency upshift and growth rate for a 700 kV CARM operated in either the TE_{11} or TE_{01} mode of cylindrical guide. Dr. Lin has performed numerical simulation of CARMs appropriate for a) EC heating of fusion plasmas and b) high power (1 kJ/μs) microwave weapons.

An experiment is being assembled to test the CARM's stability and features of efficiency enhancement and frequency upshift. A 25 kV, 2 Ω, 10 Hz, 2 μsec pulse modulator has been successfully tested. An 800 kV, 20:1/40:1 dual step-up transformer and a 400 kV SLAC electron gun have been received. A 60 kG superconducting solenoid with an extra uniform region for gyroresonant velocity transformation has been ordered. The proof of principle experiment will be performed at 33 GHz with an expected output power of 10 MW including the deleterious effect of a 1% axial velocity spread and a 52% guiding center spread, as predicted by Dr. Lin's simulations.

III. Cherenkov Cyclotron Autoresonance Maser

Velocity transformation in an improved gyroresonant wiggler has been measured. A thin pencil electron beam passed through a small aperture before propagating through the wiggler on its way toward a Uranium glass scintillation plate. The fluorescent image of the resultant electron ring yielded a direct measurement of the electron's Larmor radius from which the transverse velocity can be deduced since the magnetic field is known. The dependence of the final $v_\perp$ on the background axial magnetic field and the wiggler's transverse magnetic field has been compared to simulation results. Agreement is very good.

The Cherenkov CARM experiment was then performed with a 4 A, 90 keV beam. The wiggler fields were adjusted so that the electron had an α of 0.9 in the CARM region. The CARM's magnetic field was then swept so that the cyclotron resonance line intersected many different HE_{11} modes of the structure. A peak power of 24.6 kW was generated for the fourth order axial mode. The 15th order mode, which is near the light-line ($\omega/ck_z = 0.94$), was excited with an output power of 300 W. It is felt that the low level of output power is due to axial velocity spread. Steps are presently being taken to reduce the spread significantly (x4).

Before settling on the gyroresonant wiggler to transform the input pencil electron beam into the desired helical beam, we tested a magnetic kicker. The electron beam was passed through an iron ring within the magnetic field. The ring produces an non-adiabatic depression in the field. The $v_z B_r$ azimuthal force produces the needed transverse velocity. Unfortunately, we expect that the α of the electron beam is a strong function of radius since B_r is a first order modified Bessel function. Yet, this configuration has produced a beam with a quality good enough to excite a gyrotron cavity. The transformed 500 kW beam was directed through a gyrotron cavity (no dielectric) with a radius and length of 0.871 cm and 8.712 cm, respectively. Approximately 20 kW has been emitted at 10.5 GHz form the cavity's TE_{11} mode. The measured start of oscillation current suggests that the α of the beam was roughly 0.9. Of much interest, monochromatic second harmonic emission occurs at the 1 kW power level at 16.9 Ghz, which corresponds to the TE_{21} mode. Second harmonic emission is predicted to peak for electrons on axis for the TE_{21} mode. Similarly, the third harmonic should peak for electrons on axis for the TE_{31} mode.

AFOSR PROGRAM MANAGER: Dr.RobertBarker

Publications and Presentations (Aug. 1. 1987 - Dec. 31, 1988):

"A Cherenkov Cyclotron Autoresonance Maser," D.B. McDermott, Haibo Cao and N.C. Luhmann, Jr., *Int. J. Electronics*, 65, 477 (1985).

"Prebunched High Harmonic Gyrotron," C.S. Kou, D.B. McDermott and N.C. Luhmann, Jr., *Bull. Am. Phys. Soc.*, 32, 1864 (1987).

"Cyclotron Autoresonant Maser (CARM) Heating Source for High Field Tokamaks," N.C. Luhmann, Jr., A.T. Lin, and D.B. McDermott. *Bull. Am. Phys. Soc.*, 32, 1865, (1987).

"A Cherenkov CARM," *Bull. Am. Phys. Soc.*, 32, 1865 (1987).

"Cyclotron Autoresonance Maser (CARM) EC Heating Source for High Field Tokamaks," A.T. Lin, N.C. Luhmann, Jr., D.B. McDermott and K.R. Chu, Invited Paper, *Digest of Twelfth Int. Conf. IR & mm-Waves*, Orlando, Florida, 1987.

"Initial Operation of a Cherenkov Autoresonance Maser," H. Cao, D.B. McDermott and N.C. Luhmann, Jr., 1988 IEEE Int. Conf. Plasma Science, Seattle, Washington, 1988.

"Operation of a Prebunched High Harmonic Cyclotron," C.S. Kou, K.J. Knudsen, D.B. McDermott and N.C. Luhmann, Jr., 1988 IEEE Int. Conf. Plasma Science, Seattle, Washington.

"Initial Operation of a Cherenkov CARM," H.B. Cao, D.B. McDermott and N.C. Luhmann, Jr., *Bull. APS*, 33, 2083 (1988).

"Prebunched High Harmonic Gyrotron," C.S. Kou, D.B. McDermott and N.C. Luhmann, Jr., *Bull. APS*, 33, 2083 (1988).

"Cyclotron Autoresonant Maser (CARM) EC Heating Source for High Field Tokamaks," Q.S. Wang, A.T. Lin, N.C. Luhmann, Jr., D.B. McDermott and K.R. Chu, *Bull. APS*, 33, 2085 (1988).

"Initial Operation of a Cherenkov CARM," H.B. Cao, D.B. McDermott and N.C. Luhmann, Jr., *Digest of Thirteenth Int. Conf. IR & mm-Waves*, Honolulu, Hawaii, (1988).

"CARM EC Heating Source for High Field Tokamaks," Q.S. Wang, A.T. Lin, N.C. Luhmann, Jr., D.B. McDermott and K.R. Chu, *Digest of Thirteenth Int. Conf. IR & mm-Waves*, Honolulu, Hawaii, (1988).

"Prebunched High Harmonic Gyrotron," C.S. Kou, D.B. McDermott and N.C. Luhmann, Jr., *Digest of Thirteenth Int. Conf. IR & mm-Waves*, Honolulu, Hawaii, (1988).

"Initial Operation of a Cherenkov CARM," H.B. Cao, D.B. McDermott and N.C. Luhmann, Jr., submitted to SPIE's Symp. on Microwave and Particle Beam Sources and Directed Energy Concepts, Los Angeles, Calif., (1989).

"Cyclotron Autoresonant Maser (CARM) EC Heating Source for High Field Tokamaks," Q.S. Wang, A.T. Lin, N.C. Luhmann, Jr., D.B. McDermott and K.R. Chu, submitted to SPIE's Symp. on Microwave and Particle Beam Sources and Directed Energy Concepts, Los Angeles, Calif., (1989).

"Prebunched High Harmonic Gyrotron," C.S. Kou, D.B. McDermott, N.C. Luhmann, Jr., submitted to SPIE's Symp. on Microwave and Particle Beam Sources and Directed Energy Concepts, Los Angeles, Calif, (1989).

"CARM EC Heating Source for High Field Plasmas," Q.S. Wang, A.T. Lin, N.C. Luhmann, Jr., D.B. McDermott, and K.R. Chu, submitted to 1989 Int. Conf. on mm-Wave and FIR Technology, Beijing, China.

"Initial Operation of a Cherenkov CARM," H.B. Cao, D.B. McDermott and N.C. Luhmann, Jr., submitted to 1989 Int. Conf. on mm-Wave and FIR Technology, Beijing, China.

I. Summary of Progress

Until June, 1986 the sole goal of our AFOSR sponsored research was the theoretical and experimental investigation of the harmonic gyrotron in which the interaction occurs between large orbit, axis-encircling electrons and high order azimuthal cavity TE modes. The program encompassed both the basic device physics as well as the actual construction, testing and optimization of practical sources. The major thrust of the program was aimed toward basic research on compact high frequency sources which employ simple technology: 1) low voltage; 2) and conventional, or, ideally, permanent magnets rather than superconducting magnets, Bitter magnets or pulsed solenoids. The program philosophy stressed basic studies employing analytic and numerical calculations together with well-defined experimental measurements to elucidate the important features of the device physics.

A) High Harmonic Gyrotron Start of Oscillation (Theoretical)

We have investigated and developed the high harmonic gyrotron[1–4] which produces high frequency radiation with low magnetic fields. It is based on the synchronism of axis-encircling electrons with a high order azimuthal TE_{n11} mode, which occurs when $\omega = n\Omega_c$, where $\Omega_c = eB/\gamma m_o C$ is the relativistic cyclotron frequency and $\gamma = 1+K/m_o C^2$ where K represents the electron's energy. The requisite magnetic field is thereby reduced by n.

In this alternative gyrotron geometry, the angular phase velocity of the wave is approximately equal to the speed of light near the radial wall, so if the electrons are in synchronism with the wave, then $r_L/a \simeq v_\perp/c$, where $v_\perp$ is the perpendicular electron velocity, r_L represents the corresponding electron Larmor radius, and a is the cavity radius. Because the TE_{n11} "whispering gallery" modes are strongly localized near the radial wall, strong interaction at high harmonics requires electrons with high perpendicular energy. The filling factor, which is a measure of the interaction strength, defined as the square of the azimuthal electric field normalized to the average energy density of the mode, is shown in Fig. 1 as a function of $\beta_\perp = v_\perp/c$. Notice that an energy of approximately 500 kV is required for strong interaction at the fifteenth harmonic.

The harmonic gyrotron driven by an axis-encircling beam has been analyzed in a relativistic linear Vlasov treatment which has yielded the start-oscillation current and a qualitative value for device efficiency. The dependence of the harmonic gyrotron on parameters is strikingly similar to the conventional gyrotron. Therefore, high efficiencies can be expected as in the standard gyrotron in addition to a significant reduction in the magnetic field. The analysis has been published in The Physics of Fluids 26, 1936 (1983).

B) Gyroresonant RF-Accelerator (Experimental and Theoretical)

We have just seen that very energetic electrons (>> 100 keV) are required for strong coupling between the electron beam and the wave in a high harmonic interaction. Our experiment uses a gyroresonant RF accelerator to produce the high energy, axis encircling electron beam[5–7]. A low energy, pencil like electron beam ($\leq$ 0.5 A, $\leq$ 4 keV) is injected along the magnetic field into a cylindrical cavity which supports a large amplitude, circularly polarized TE_{111} mode at a frequency of 2.8 GHz. The resulting beam consists of a tightly wound helix of high energy ($\leq$ 500

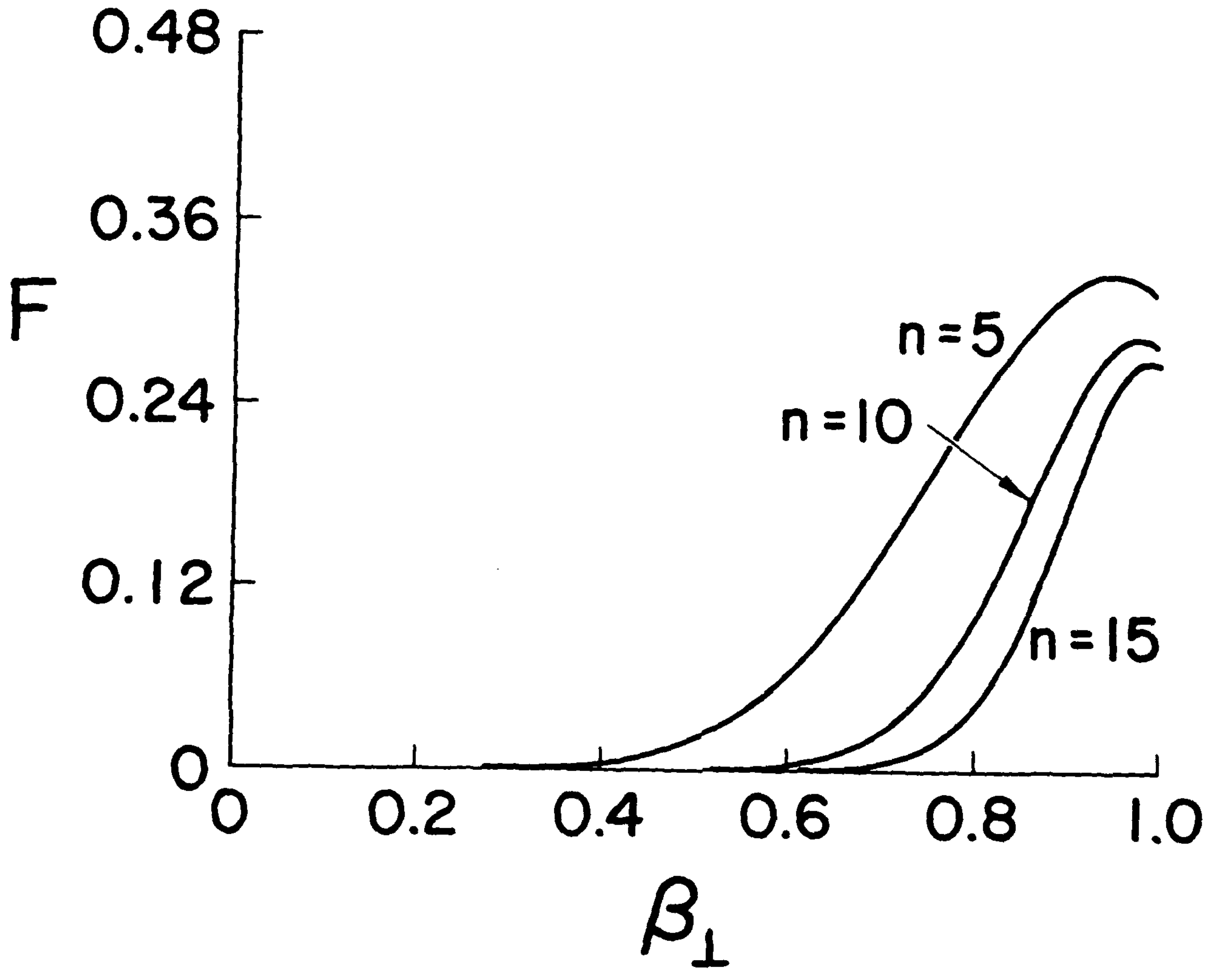

Figure 1 Dependence of the filling factor on $\beta_\perp$ for three high harmonic interactions, $\beta_\perp = v_\perp /c$.

keV) axis encircling electrons.

The harmonic gyrotron's resonance condition, which is $\omega = n\Omega_{co}/\gamma$, can be rewritten as $\omega/(n\omega_{acc}) = \Omega_{co}/(\gamma\omega_{acc})$, where ω_{acc} represents the cavity frequency, Ω_{co} = eB/mc is the rest mass cyclotron frequency. Therefore, in order to properly design the gyrotron cavity, the value for $\gamma/(\Omega_{co}/\omega_{acc})$ of the accelerated beam at the desired γ must be known. The electron energy produced in the rf-accelerator, determined by the radius of the scintillation image of the ring, as a function of magnetic tuning about the resonance condition ($\omega_{acc} = \Omega_{co}$) has been measured and plotted in Fig. 2 where it is compared with numerical simulation. The agreement is excellent - within 10%. The optimum magnetic field occurs when the rf frequency is roughly equal to the average cyclotron frequency, i.e.,

$$\Omega_{co} = \omega_{acc}(1 + \gamma)/2 \tag{1}$$

where γ represents the final electron γ and the initial γ has been taken equal to unity. Therefore, the important ratio mentioned earlier can be approximated by

$$\frac{\gamma}{(\Omega_{co}/\omega_{acc})} = \frac{2\gamma}{1+\gamma} \tag{2}$$

The results have been published in the Journal of Applied Physics 58, 4501 (1985).

C) Moderate Harmonic Emission (Experimental)

Our initial harmonic gyrotron experiments were designed to verify the theoretical predictions of start-oscillation and saturated efficiency.

The experimental start of oscillation current for the third through fifth harmonic interactions in Tube X.2 are plotted in Fig. 3 as a function of magnetic field. Referring to Fig. 4, we see that the measured starting currents are in good agreement with theory. A qualitative estimate of the maximum efficiency for transfer of electron beam energy into millimeter wave energy is given by the width of the gain function. Essentially, the electrons "walk-off" the interaction as they lose energy. The peak efficiency is given by

$$\eta = (\frac{\pi^2}{2})(\frac{1}{n})(\frac{\gamma}{\gamma-1})(\frac{v_{\parallel}}{c})(\frac{a}{L}) \tag{3}$$

where $v_{\parallel}$, a and L represent the electron's velocity along the magnetic field, the cavity radius and length, respectively. This equation also describes the high efficiency conventional gyrotron. Note that the efficiency is inversely proportional to the cavity length and harmonic number. Also, the efficiency is strongest at low energy ($\gamma \rightarrow 1$). Unfortunately, the interaction strength decreases as the beam energy is lowered. Therefore, peak efficiency must be compromised in order to achieve oscillation.

For a parametric study three cavities for moderate harmonic emission were fabricated with different lengths. In addition to obtaining quantitative agreement within 50% of theoretical predictions, both the start-oscillation current and efficiency were observed to scale properly with cavity length.

The theoretical start-oscillation current is essentially proportional to L^{-2}. Since the lengths of the three cavities (otherwise identical) are 5.08 cm, 3.81 cm and 2.54 cm, the minimum start-oscillation current should scale as 1:2.25:4. The observed third harmonic interaction actually scaled as 1:3:4 and the fourth harmonic interaction scaled as 1:2.5:5. The "mean agreement" is

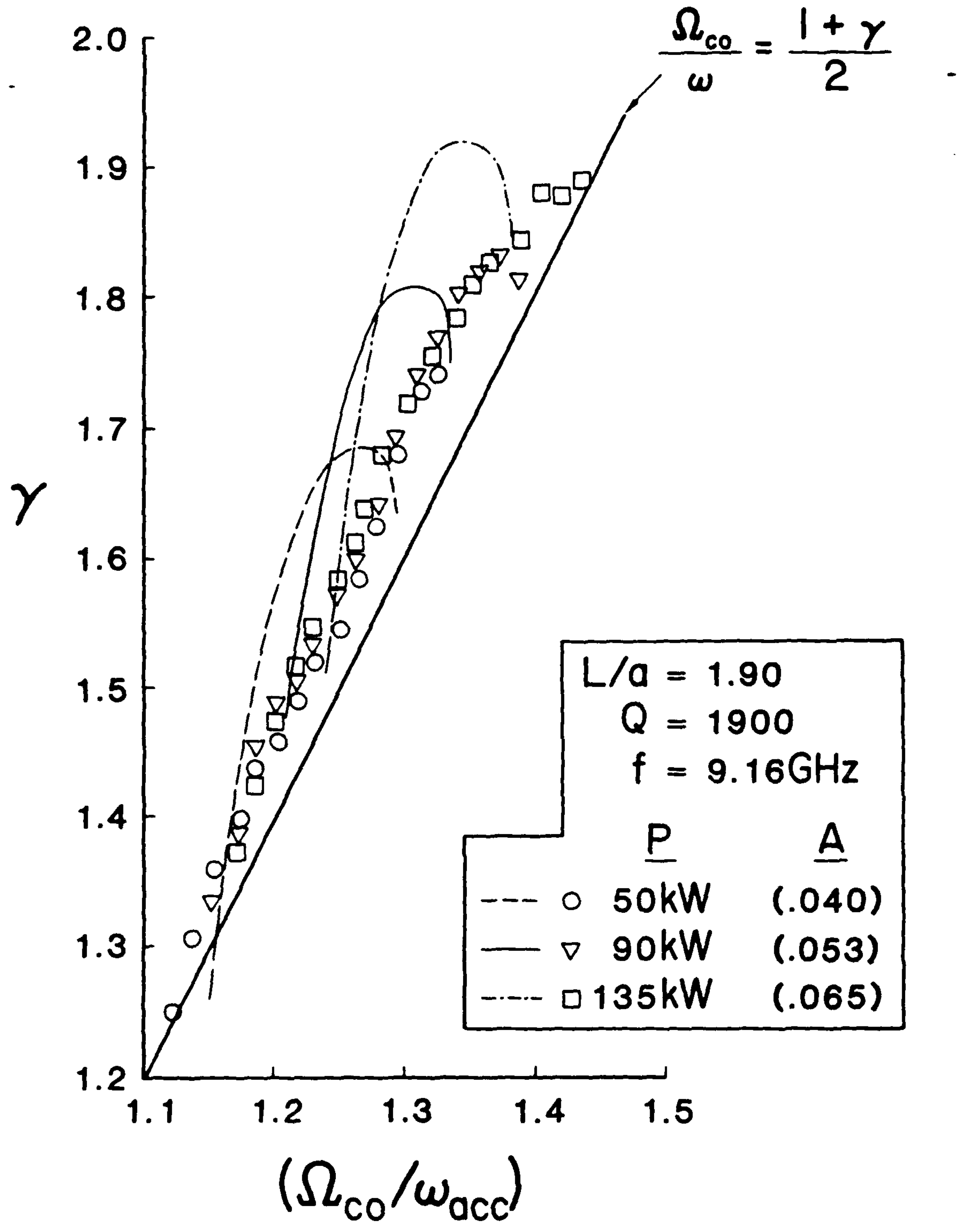

Figure 2 γ as determined by experiment (data points) and simulation (curves) for three values of rf power into the x-band accelerator.

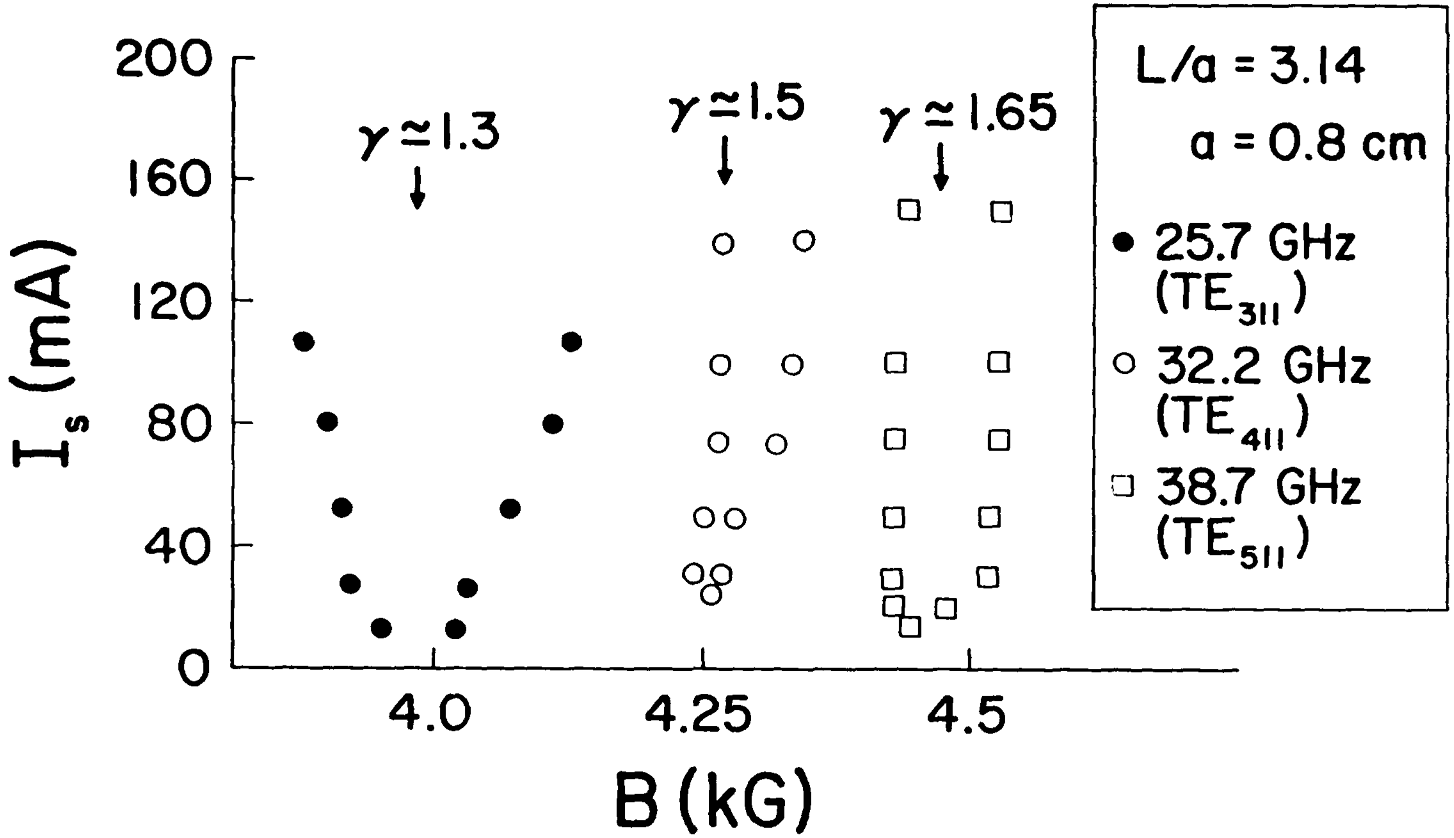

Figure 3 Measured start of oscillation current for the third (25.7 GHz), fourth (32.3 GHz) and fifth (38.7 GHz) harmonic interactions in Tube X.2.

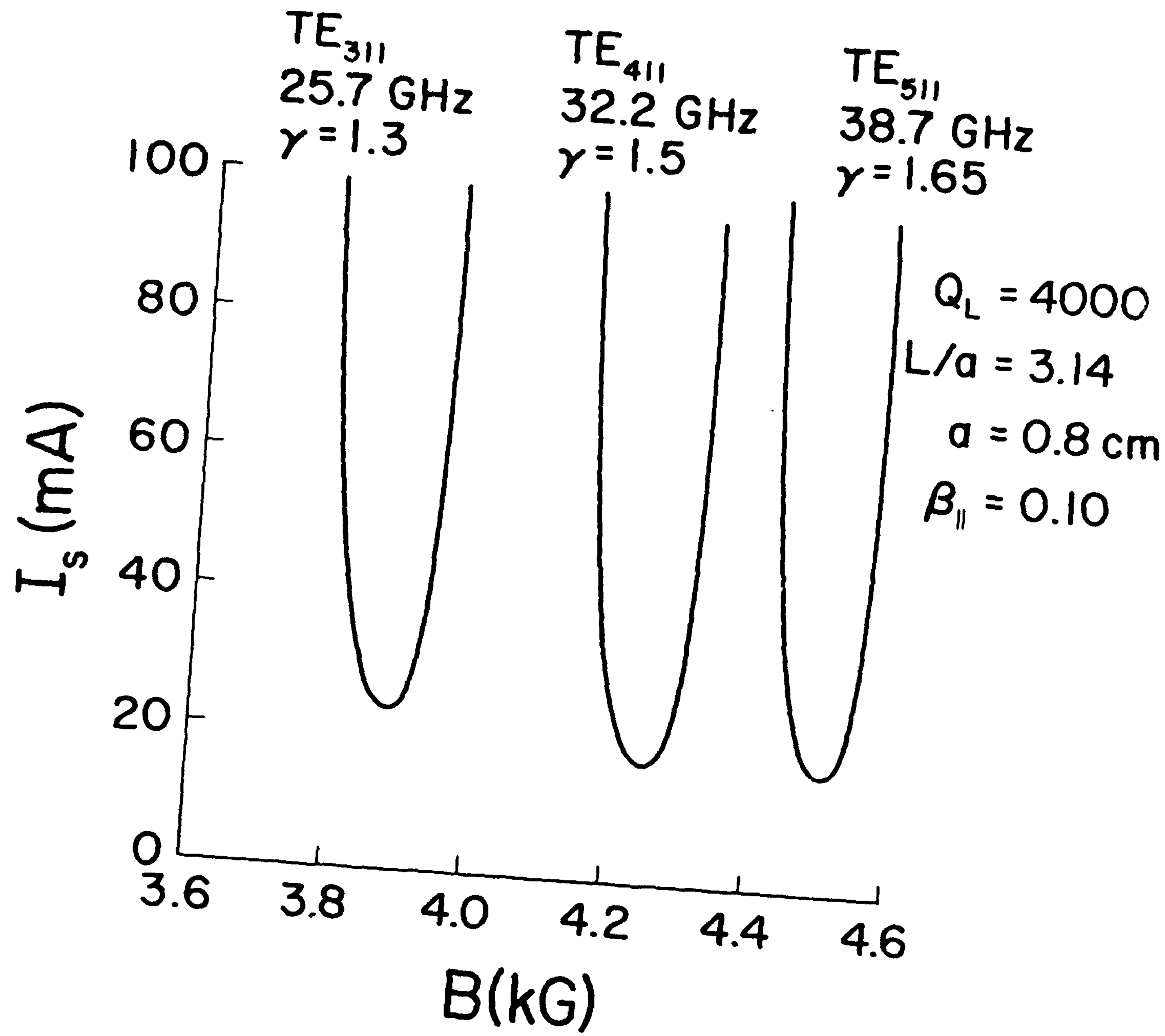

Figure 4 Theoretical start of oscillation current for Tube X.2.

therefore within 20%.

The dependence of the predicted conversion efficiency on cavity length has been verified by comparing the peak efficiency of the third harmonic interaction for the two smaller cavities. The efficiency should be inversely proportional to the cavity length (see Eq. 3). The measured values for conversion efficiency of 9.5% and 15% agree well with the predicted ratio of 1.5. Unfortunately, the measurements in the longer cavity cannot be used since this cavity was extremely undercoupled and the higher harmonic interactions in the short cavity did not saturate.

The experimental results have been published in the International Journal of Infrared and Millimeter Waves 4, 639 (1983).

D) Mode Competition

1. Axial Mode Control

We have also been successful in controlling the axial mode number, l, of the unstable wave in the gyrotron cavity. This is important because multi-mode oscillation lowers the device efficiency and is undesirable in itself. Axial mode competition is not a problem in a conventional gyrotron where the cavity's Q is inversely proportional to l^2 due to the use of diffraction coupling. In our high harmonic gyrotrons the power is coupled out through the side wall. As a result the Q is roughly independent of l. The relative frequency difference between two neighboring, low order axial modes in a relatively long cavity of practical interest is small enough that they are likely to oscillate simultaneously. This has been observed and is evident in Fig. 5 where the two lowest order axial modes oscillated for each of the third, fourth, and fifth harmonic interactions. Furthermore, the severity of axial mode competition increases for higher harmonics.

We suppressed axial mode competition by using resistive wall loading. A thin band of Eccosorb 268E absorber was applied to the midplane of the cavity. Odd axial modes are heavily damped because their intensity peaks along the midplane. In contrast, the even axial modes are relatively unaffected because a null occurs at the midplane. The current at the threshold for oscillation for the cavity corresponding to Fig. 5, but which has been sliced through the axis for azimuthal mode control and filled with a lossy ring along its midplane, is shown in Fig. 6. The emission was monochromatic as desired. Furthermore, the conversion efficiency increased to 16% while 2 kW at 33 GHz was emitted.

2. Complex Cavity

During the past year we have attempted to operate a complex cavity for the purpose of the suppression of mode competition. A complex cavity[8] is comprised of two or more cavities such that only one frequency is resonant in both cavities. This complex mode extends over a longer length than the modes localized in just one cavity. Thus the start-oscillation current for this frequency is much lower than the start-oscillation current for the other frequencies. Consequently, the complex mode will saturate before the other modes even begin to oscillate. In a harmonic gyrotron complex cavity driven by axis-encircling electrons the modes in each cavity must have the same azimuthal number.

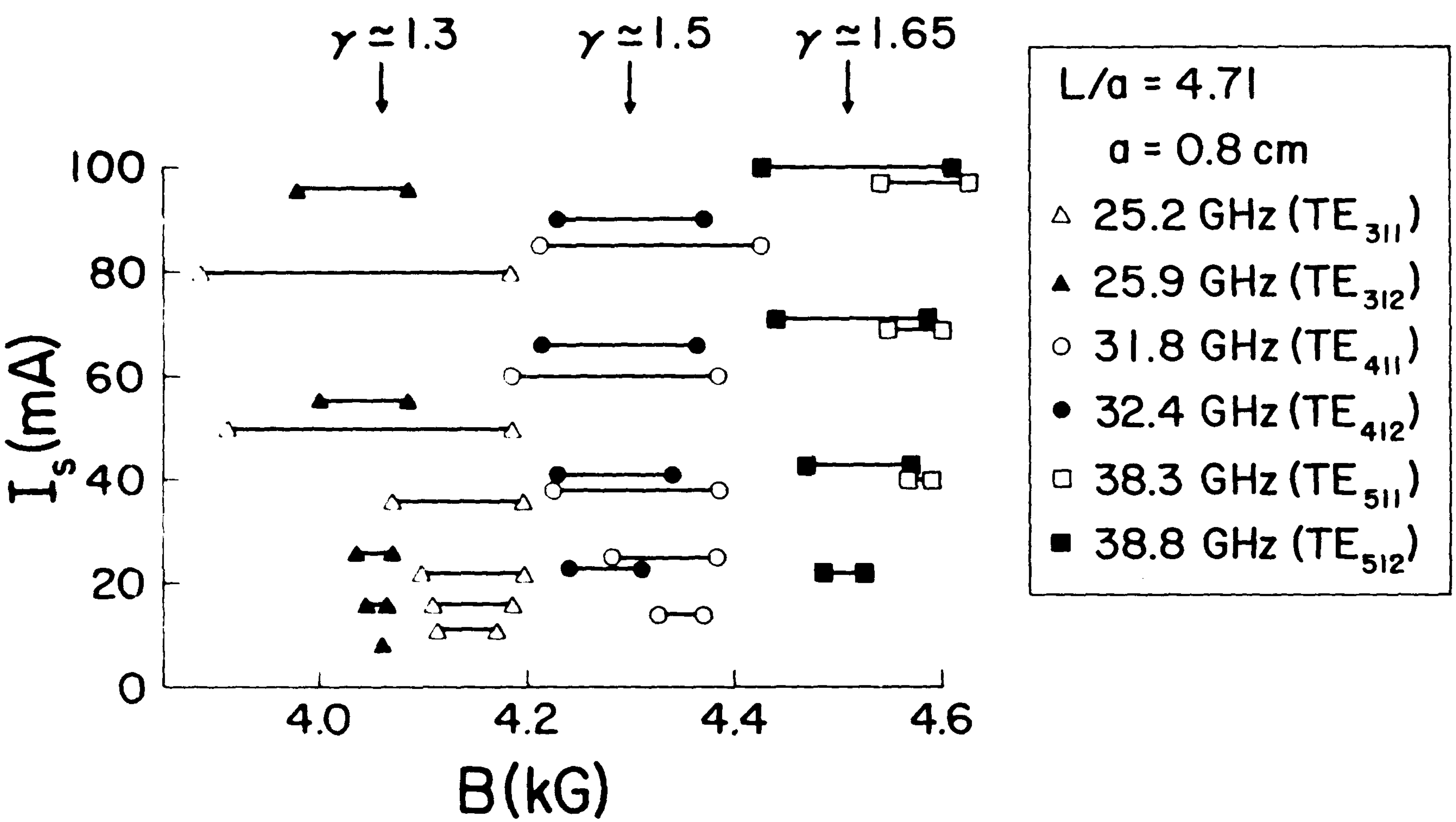

Figure 5 Measured start of oscillation current for the third, fourth and fifth harmonic interactions in Tube X.3. The two lowest axial modes oscillated simultaneously for each harmonic.

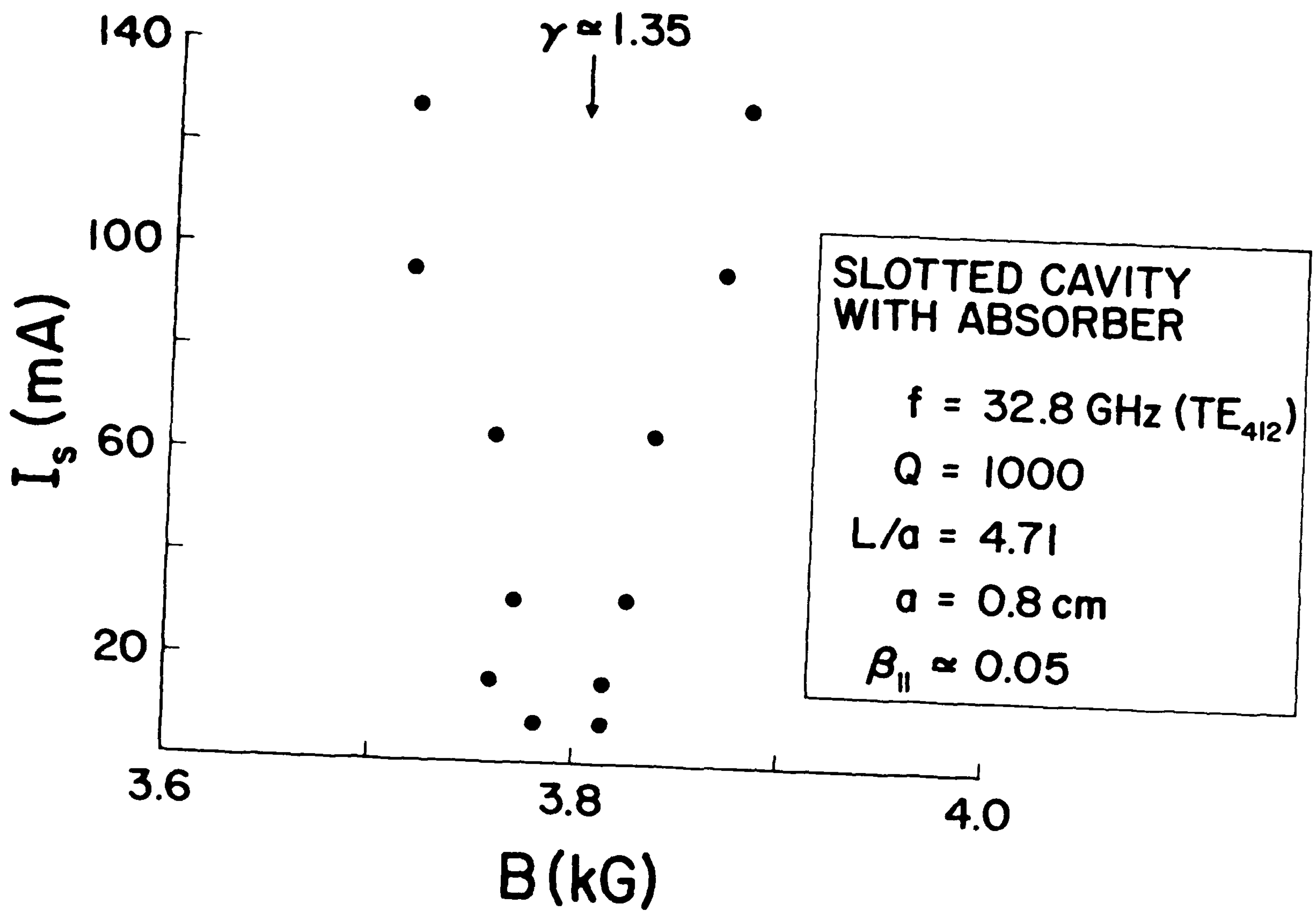

Figure 6 Measured start of oscillation current for Tube X.5, which is similar to Tube X.3 (see Fig. 4) except that it has been sliced through the axis and includes a lossy dielectric ring along the midplane. The resulting emission was monochromatic.

We have successfully developed a theory for the optimum design of a complex cavity. The rule is that the start oscillation current (I_s) for each cavity should be equal. This yields the greatest possible difference between I_s for the complex mode and I_s of the modes isolated in either cavity. Since I_s is inversely proportional to the square of the interaction length, I_s for the complex mode will be four times lower than that of any other mode. Therefore, the electron beam will lock onto and saturate this complex mode before the others even begin to oscillate.

Assuming that the resonance condition, $\omega \geq n\Omega_c$, is properly satisfied the start oscillation current of a TE_{nmp} mode in an nth harmonic gyrotron can be written

$$I_s = \left[1-\left(\frac{n}{q_{nm}}\right)^2\right]\left[\frac{aJ_n(q_{nm})}{l}\right]\frac{W}{Q} \tag{4}$$

where q_{nm} is the mth zero of the nth-order Bessel function, $J_n(y)$; l, a and Q are the cavity's length, radius and quality factor, respectively, and W represents a product of parameters which are independent of the cavity mode. If the two constituents of the complex cavity are a TE_{821} mode and a TE_{811} mode, and the two Qs are equal, then the TE_{821} cavity should be three times the length of the TE_{811} cavity.

E) High Harmonic Emission (Experimental)

Once the theory of the high harmonic gyrotron was verified, we felt confident to assemble a higher harmonic experiment. We achieved 56 and 65 GHz operation at 100 W levels. Much experimental difficulty was encountered at these high frequencies because the transmission of the output window at high frequencies was very poor.

F) Prebunched High Harmonic Gyrotron

In this interaction the electrons radiate at harmonics of the rf accelerator's resonant frequency. The efficiency will be extremely high because all electrons lose energy to the wave and this is a lower order interaction than the gyrotron where some of the electrons actually gain energy from the cavity fields. It depends on the fact that the rf accelerator produces a phase bunched beam as it accelerates. In essence the rf accelerator behaves like the buncher cavity of a klystron. However, a tremendous advantage exists here because the bunched beam loses energy to a traveling wave in the catcher cavity rather than a standing wave. Consequently, transit time effects do not occur. Therefore, the catcher cavity can be large resulting in a potentially high power millimeter wave source.

An important feature of the accelerated beam has not yet been exploited: The accelerator produces a bunched beam. The accelerator transforms an input pencil beam into a corkscrew beam, which implies azimuthal bunching. This free energy can be tapped if the beam then progresses through a second cavity where it interacts with the nth order azimuthal TE_{n1} mode. Since the cavity fields are proportional to $\cos(n\theta-\omega t)$ and $d\theta/dt = \Omega_c$, electrons maintain their phase relationship with the wave if

$$\omega = n\Omega_c \tag{5}$$

as in the high harmonic gyrotron. The electrons continually enter the cavity at the optimum phase if

$$\omega = n\omega_{acc} \tag{6}$$

The electrons are then all synchronized with the decelerating phase of the wave. The entire beam loses energy to the wave. This is in contrast to the more common higher order harmonic gyrotron where some electrons lose energy to the wave while others gain energy. For both to be true the magnetic field must be tuned so that

$$\Omega_c = \omega_{acc} \tag{7}$$

This relation can be rewritten

$$\gamma = \Omega_{co}/\omega_{acc} \tag{8}$$

It is not always possible to attain Eq. 8. Under most circumstances Eq. (8) cannot be satisfied because the $v_\perp x B_\perp$ force from the wave reflects the electrons midway through the cavity. However, there exists a minimum input velocity for any accelerator input power at which the electrons can pass through the barrier. We have numerically simulated the acceleration trajectories to discover under what conditions Eq. (8) can be satisfied. Figure 7 gives the range of γ which result while satisfying Eq. (8). For an input power of 25 kW, which is roughly the minimum power from our present 9 GHz magnetron, the injected electron energy must be 15 keV. An initial cavity has been designed for emission at the fourth harmonic, 36.8 GHz. Its length is 1.27 cm.

E) Dielectric Rod (Theoretical)

We have shown that a dielectric rod aligned along the bore of a cavity can reduce the energy requirements of the electron beam for high-harmonic gyrotron operation. As seen in Fig. 8 a large interaction filling factor can occur at high harmonics for moderate-energy electrons (~ 80 keV) spiralling around the rod within the evanescent region of a high order azimuthal dielectric waveguide mode. Since the magnetic field strength is reduced by an order of magnitude in an interaction at the tenth harmonic of the cyclotron frequency, a submillimeter-wave gyrotron is now truly feasible because the acceleration voltages can be conveniently produced by DC power supplies. The analysis has been published in the International Journal of Infrared and Millimeter Waves 4, 831 (1983).

H) Cherenkov Cyclotron Autoresonance Maser

The CARM[9,10] is a novel variation of the cyclotron maser. It is designed so that the electrons remain in synchronism with the wave even as they lose energy. The resonance condition, as for all fundamental gyro-devices, is

$$\omega = k_z v_z + \frac{\Omega_{co}}{\gamma} \tag{9}$$

where k_z and v_z are the axial wavevector and velocity, respectively. Resonance can be maintained if the longitudinal velocity decreases at the same rate as the energy. The dynamic phase shift of an electron relative to the wave is

$$\Delta\phi = \left[k_z \Delta v_z + \Omega_c \Delta\left(\frac{1}{\gamma}\right) \right] \tau \tag{10}$$

where τ is the growth rate of the interaction. Using the relation between momentum and energy loss during a radiative process, the phase variation can be written as

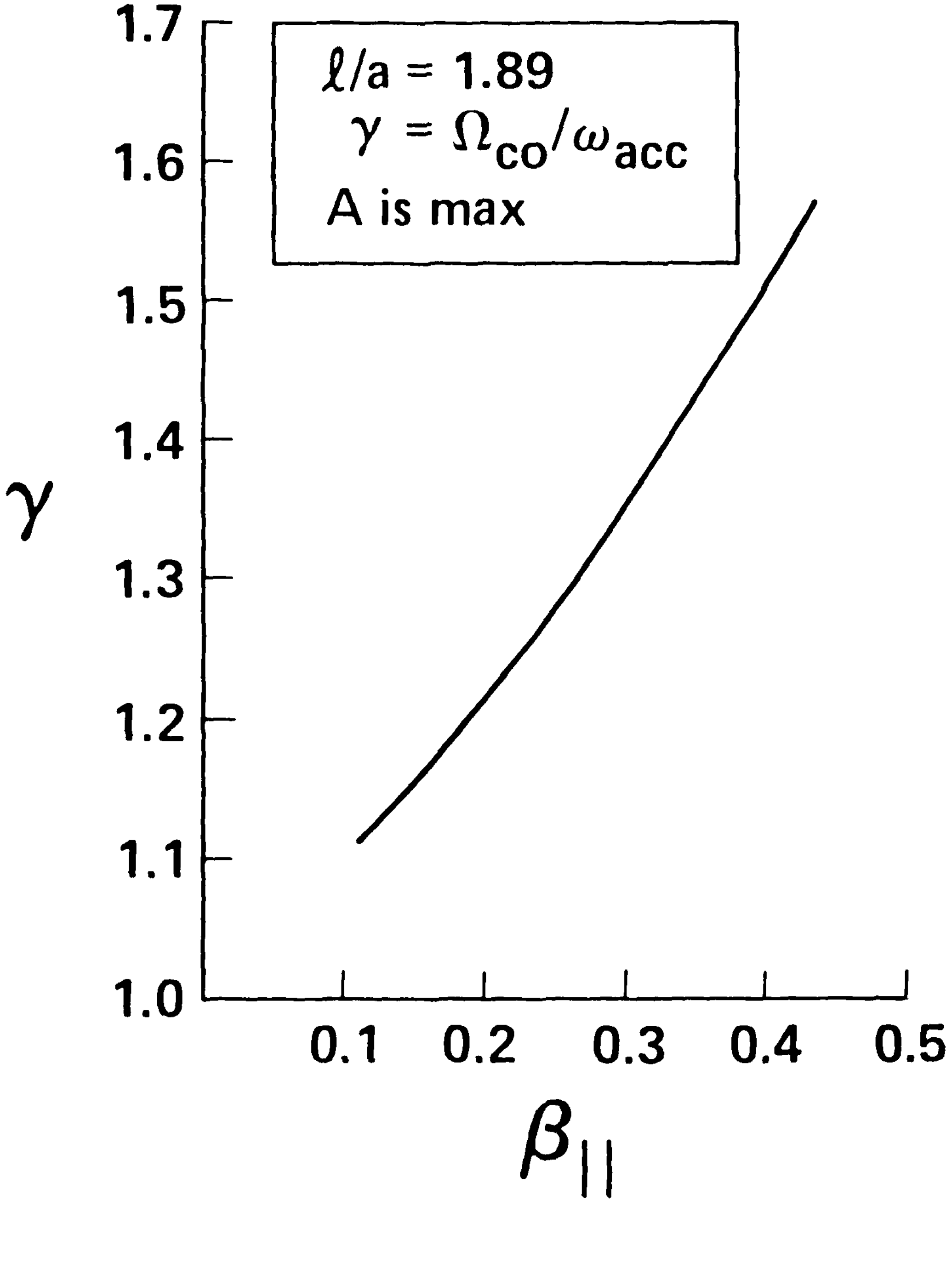

Figure 7 Maximum accelerated γ as a function of injected axial velocity for system satisfying the prebunched gyrotron condition.

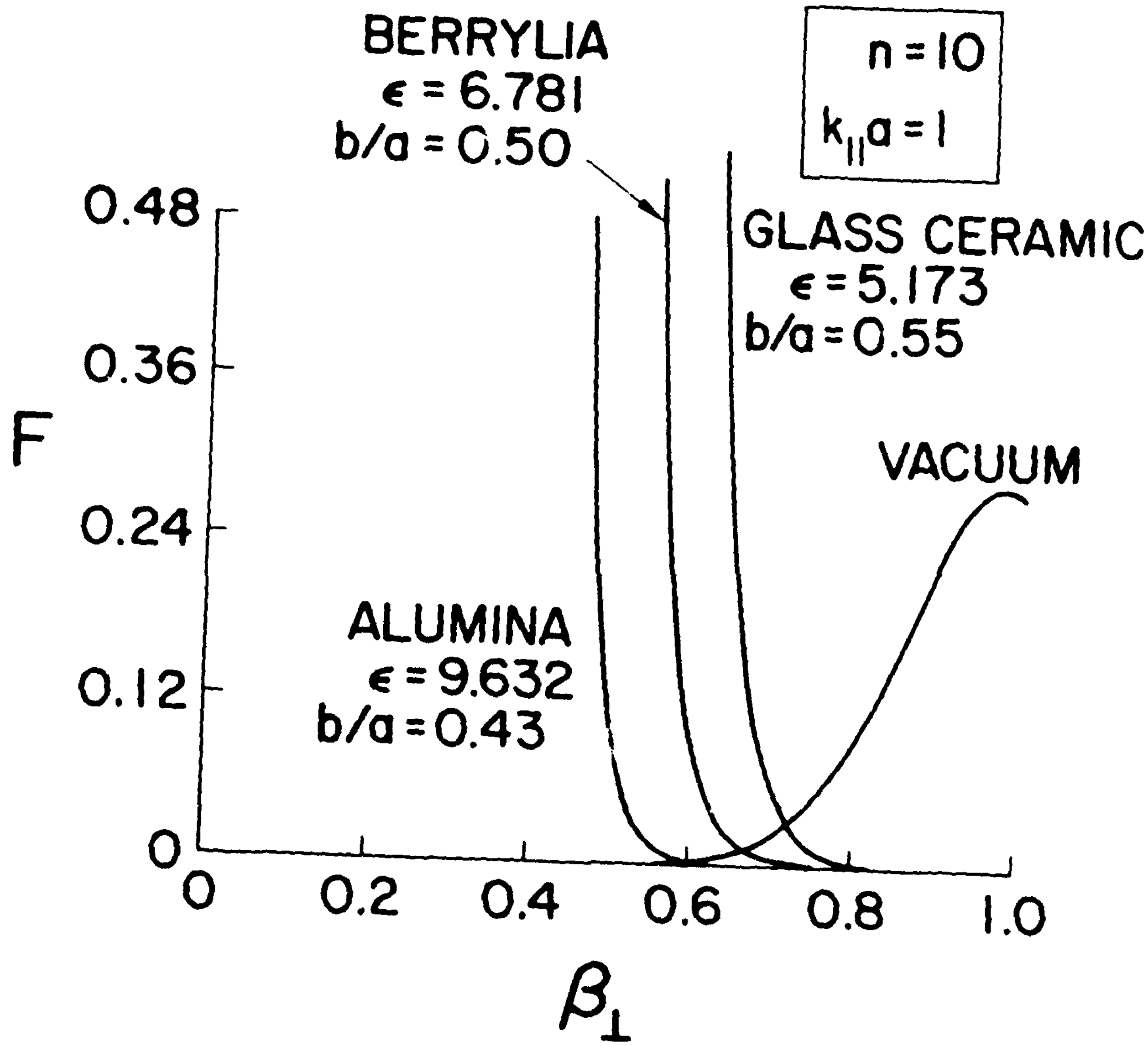

Figure 8 The dependence of the filling factor, or interaction strength, on the transverse velocity for the lowest order mode in a berrylia, alumina, and glass ceramic rod at the tenth harmonic. Also shown is the vacuum case.

$$\Delta\phi = \frac{\Delta\gamma}{\gamma}\omega\tau\left[\beta_{ph}^{-2} - 1\right] \quad (11)$$

where $\beta_{ph} = \omega/ck_z$. Notice that phase slippage occurs less slowly as β_{ph} approaches unity. This interaction can thereby yield a very high efficiency for particle to wave energy transfer.

Resonance with a fast wave ($\beta_{ph} > 1$) while avoiding the excitation of an absolute instability is most readily achieved by a highly relativistic beam, which can also exploit another feature of the CARM. The output frequency is Doppler-upshifted to

$$\omega = (1 - \beta_z)^{-1}\,\Omega_c \quad (12)$$

An upshift of four has been achieved in a CARM which has emitted 10 MW at 125 GHz.[11]

Relativistic electrons are unnecessary if a slow wave structure is used. An appreciable upshift of the frequency can still occur since the axial velocity is effectively increased by the structure's refractive index.

A slow-wave CARM amplifier whose guiding structure is a dielectric cylinder within the metallic tube is of significant interest. Shown in Fig. 9 is the dispersion relation of the hybrid TE_{11} mode within several polythylene tubes of varying thickness derived from the theory of Ref. 12. The experimentally measured frequencies of the lowest order axial hybrid TE_{11} modes in several cylindrical cavities of varying length are included.

This geometry has the fortuitous feature that the rf field is a null throughout the dielectric when $\beta_{ph} = 1$. The radial dependence of the filling factor, defined as the square of the perpendicular rf electric field normalized to the average energy density, is plotted in Fig. 10 for several values of wavevector including the wave with $\beta_{ph} \approx 1$. Notice that the rf fields on the axis are actually enhanced by the presence of the dielectric. This is corroborated by Fig. 11, where the filling factor at several radial positions is plotted as a function of wavevector. The value of the field on axis is a maximum and near the dielectric is a minimum for $\beta_{ph} = 1$. Thus the wave is strong in the central vacuum region for the values of phase velocity which yield the highest efficiency.

Since the fields peak on axis, the electron gun geometry most appropriate for this tube is a pencil beam which acquires its perpendicular motion by passing through a bifilar undulator at gyroresonance,

$$R \equiv \frac{\lambda_u \Omega_{co}}{2\pi\gamma v_z} = 1 \quad (13)$$

where λ_u is the undulator's wavelength, as depicted in Fig. 12. The periodic transverse magnetic field of the undulator will couple the transverse velocity to the axial velocity.

We have numerically simulated the motion of electrons in the gyroresonant undulator. Electrons were injected axially into the periodic transverse magnetic field where the periodic $v_\parallel \times B_\perp$ force drives them at their natural frequency, the cyclotron frequency, if Eq. 13 is satisfied. The value of $\alpha = v_\perp / v_\parallel$ at the exit of a ten period undulator as a function of the wiggler field amplitude for a 75 keV electron is shown in Fig. 13 for several values of initial resonance ratio, R. An initial resonance ratio of unity (Eq. 13 is satisfied) yields the most rapid increase in $v_\perp$, but α saturates at 0.4. However, since the resonance condition is a function of a varying v_z, a value for R less than one yields a final α far in excess of 0.4.

The differential equations governing the forced resonant motion can be solved analytically for the linear regime, valid if v_z does not vary appreciably. For exact resonance (R=1) the

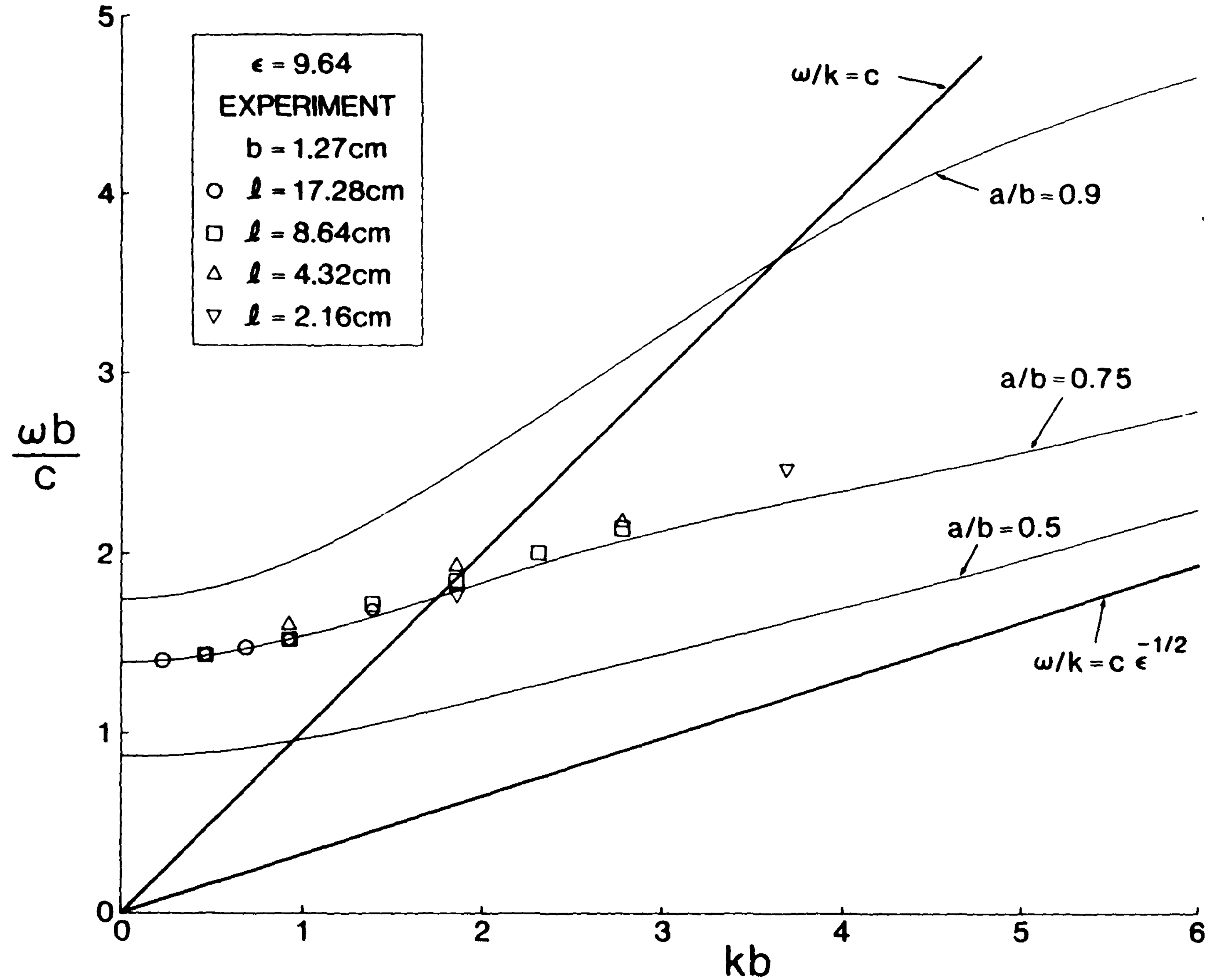

Figure 9 Dispersion of hybrid TE_{11} wave in polythylene loaded cavity including experimental measurements with inner to outer diameter ratio, a/b, of 0.75 for several cavity lengths.

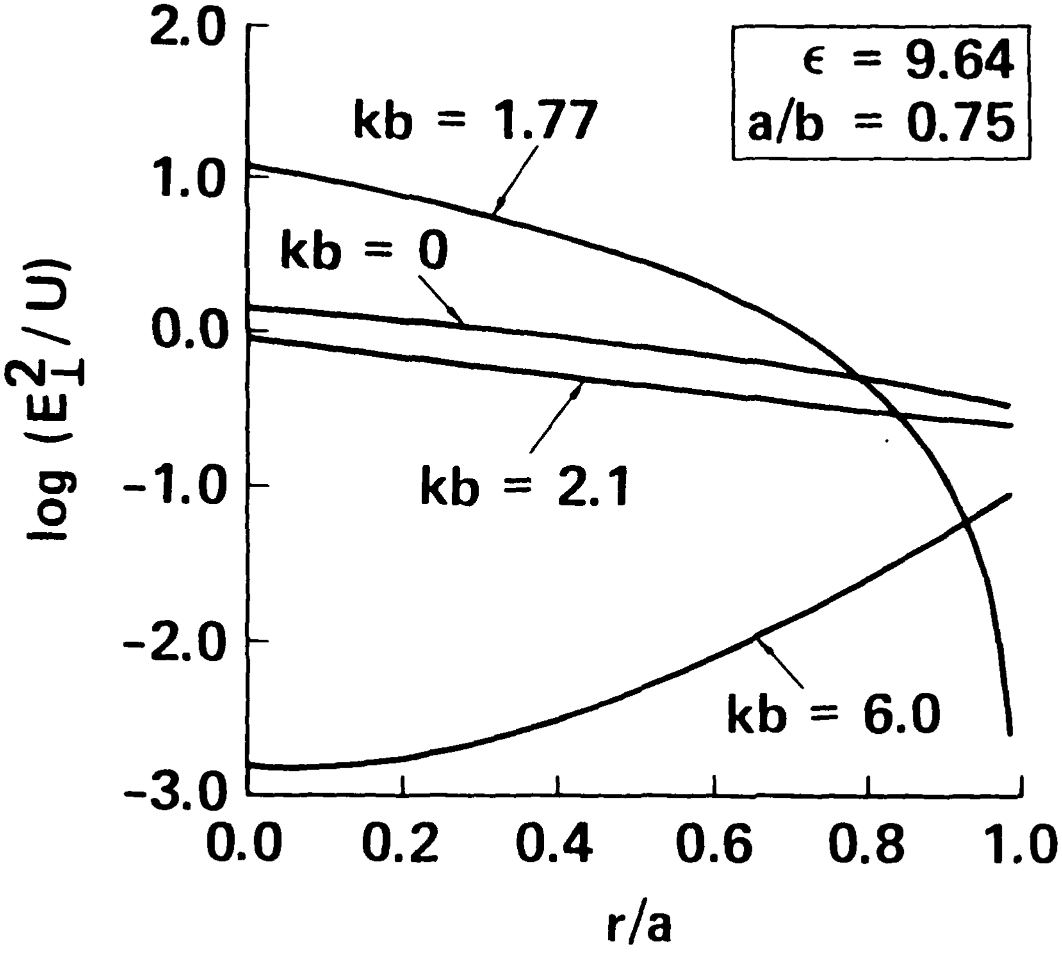

Figure 10 Radial dependence of the normalized perpendicular electric field squared for several values of wavevector for a polythylene tube with a/b = 0.75. $\beta_{ph} = 1$ for kb = 3.75

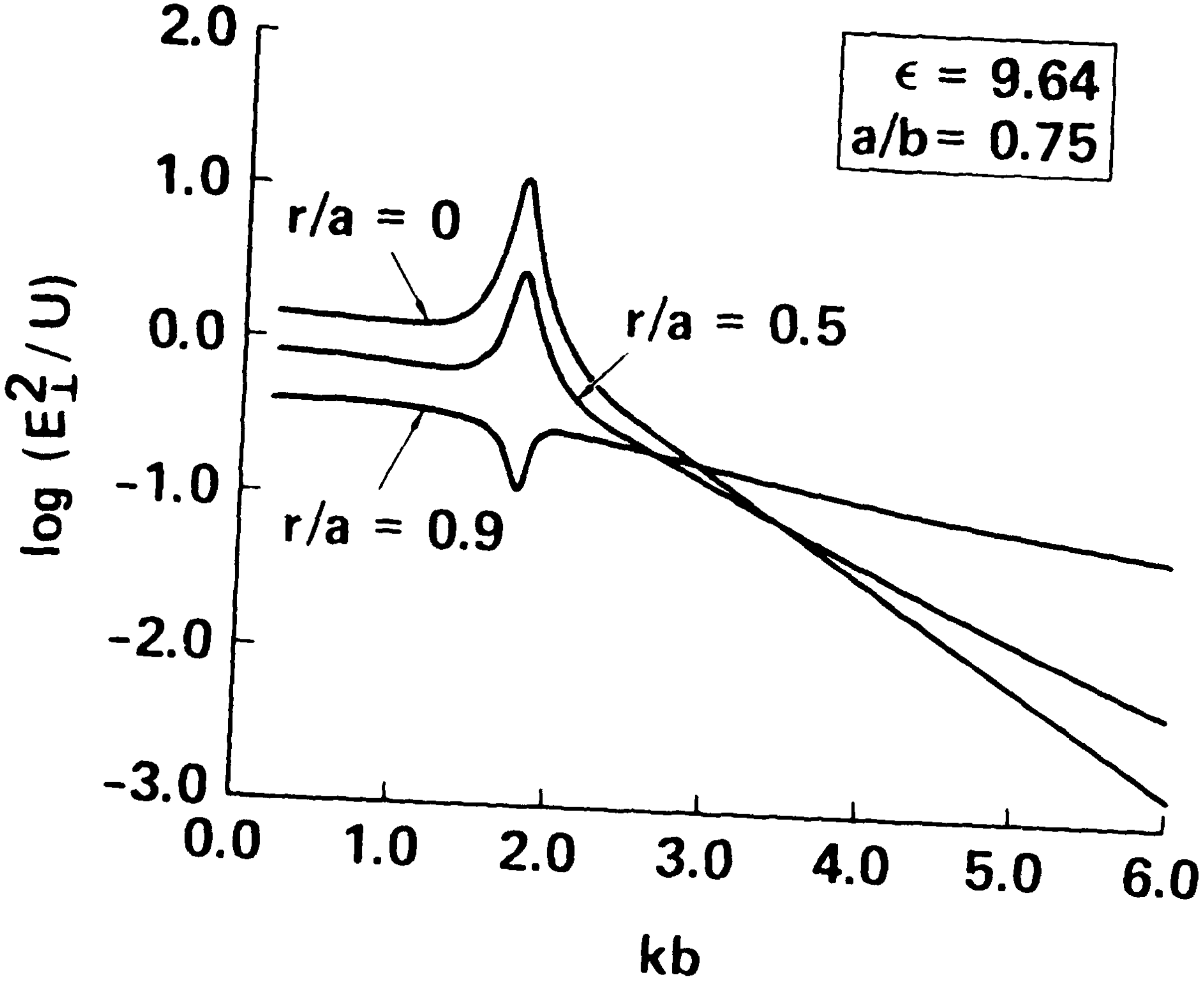

Figure 11 Dependence of the normalized perpendicular electric field squared on the wavevector for a polythylene tube with a/b = 0.75. $\beta_{ph} = 1$ for kb = 3.75.

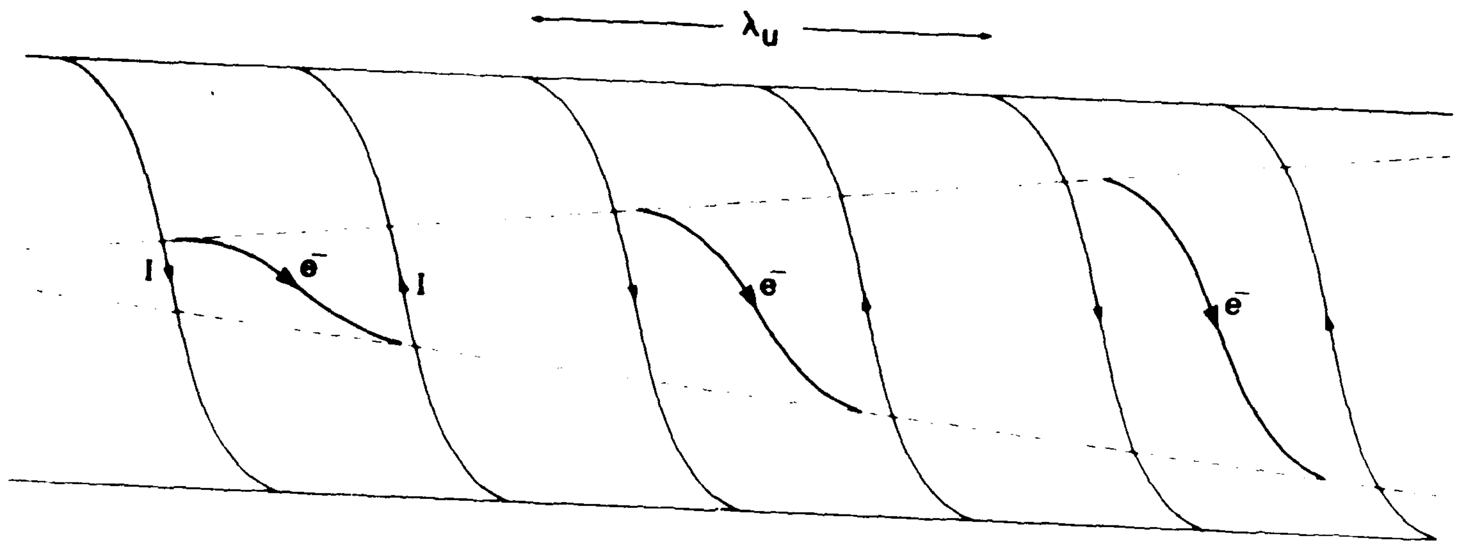

GYRO – RESONANCE: $V_Z = f_c \lambda_u$

$$\longrightarrow V_\perp = \left(\frac{eB_u}{\gamma mc}\right) Z$$

Figure 12 Trajetory of electron gyroresonant with bifilar helix.

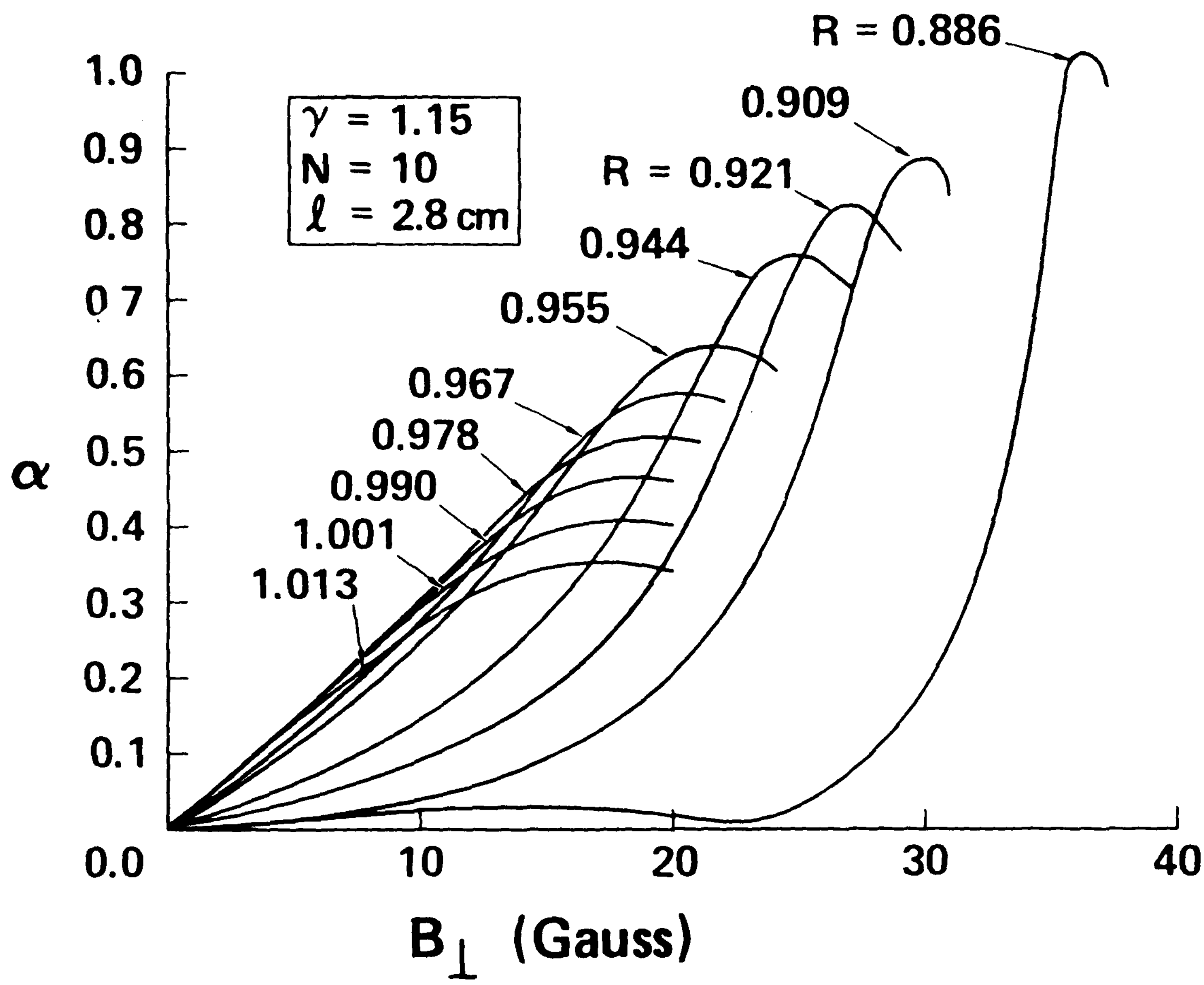

Figure 13 Dependence of final $v_\perp / v_\parallel$ on wiggler field amplitude for 75 keV electron injected axially into ten period undulator for several values of resonance ratio.

transverse velocity grows linearly, given by

$$v_\perp = \left(\frac{eB_\perp}{\gamma mc}\right)z \tag{14}$$

where $B_\perp$ is the amplitude of the wiggler's field. This analytical relation accurately describes the numerical results for weak $B_\perp$.

The motion of particles in the Cherenkov wave is being simulated. In addition to the competing mechanisms of axial and azimuthal bunching, the transverse magnetic component of the wave, which is equal to the transverse electric component for $\beta_{ph} = 1$, may aggravate the bunch formation and lower the conversion efficiency.

The culmination of this investigation will be a Cherenkov CARM amplifier. However, preceding this experiment will be the realization of Fig. 14 in a simpler configuration, that of an oscillator. Even before a Cherenkov CARM oscillator is built, a conventional fast-wave gyrotron will be tested. The theory for the gyrotron interaction is well understood and will allow us to test most of the components, especially the gyroresonant wiggler. The start of oscillation current for the TE_{111} mode will be 1A for a 75 keV beam with an α of 0.8 when the cavity has a quality factor (Q) of 1700 and a length to radius ratio of 10. The efficiency of transverse energy conversion is expected to be 25%, but because of the low α the total efficiency will be only 10% yielding an output power of 40kW. Since the beam parameters were chosen to optimize the Cherenkov CARM, they cannot be expected to yield good gyrotron performance, i.e. high efficiency. Yet we feel this experiment is very worthwhile because the major components can thereby be tested in a relatively controlled environment. In addition, this experiment will give us time to perform the analytical theory of the Cherenkov CARM to determine the desired cavity length. All components have been fabricated and we have just begun to hot test the system.

REFERENCES

1. D.B. McDermott, N.C. Luhmann, Jr., A. Kupiszewski and H.R. Jory, Phys. Fluids 26, 1936 (1983).

2. D.B. McDermott, N.C. Luhmann, Jr., D.S. Furuno, A. Kupiszewski and H.R. Jory, Int. J. Inf. and mm-Waves 4, 639 (1983).

3. D.S. Furuno, D.B. McDermott, N.C. Luhmann, Jr., and P. Vitello, Int. J. Elec. 57, 1151 (1984).

4. K.R. Chu, D.S. Furuno, N.C. Luhmann, Jr., D.B. McDermott, P. Vitello and K. Ko, IEEE Trans. Plasma Science 13, 435 (1985).

5. H.R. Jory and A.W. Trivelpiece, J. Appl. Phys. 39, 3053 (1968).

6. N.C. Luhmann, Jr. and A.W. Trivelpiece, Phys. Fluids 21, 2039 (1978).

7. D.B. McDermott, D.S. Furuno and N.C. Luhmann, Jr., J. Appl. Phys. 58, 4501 (1985).

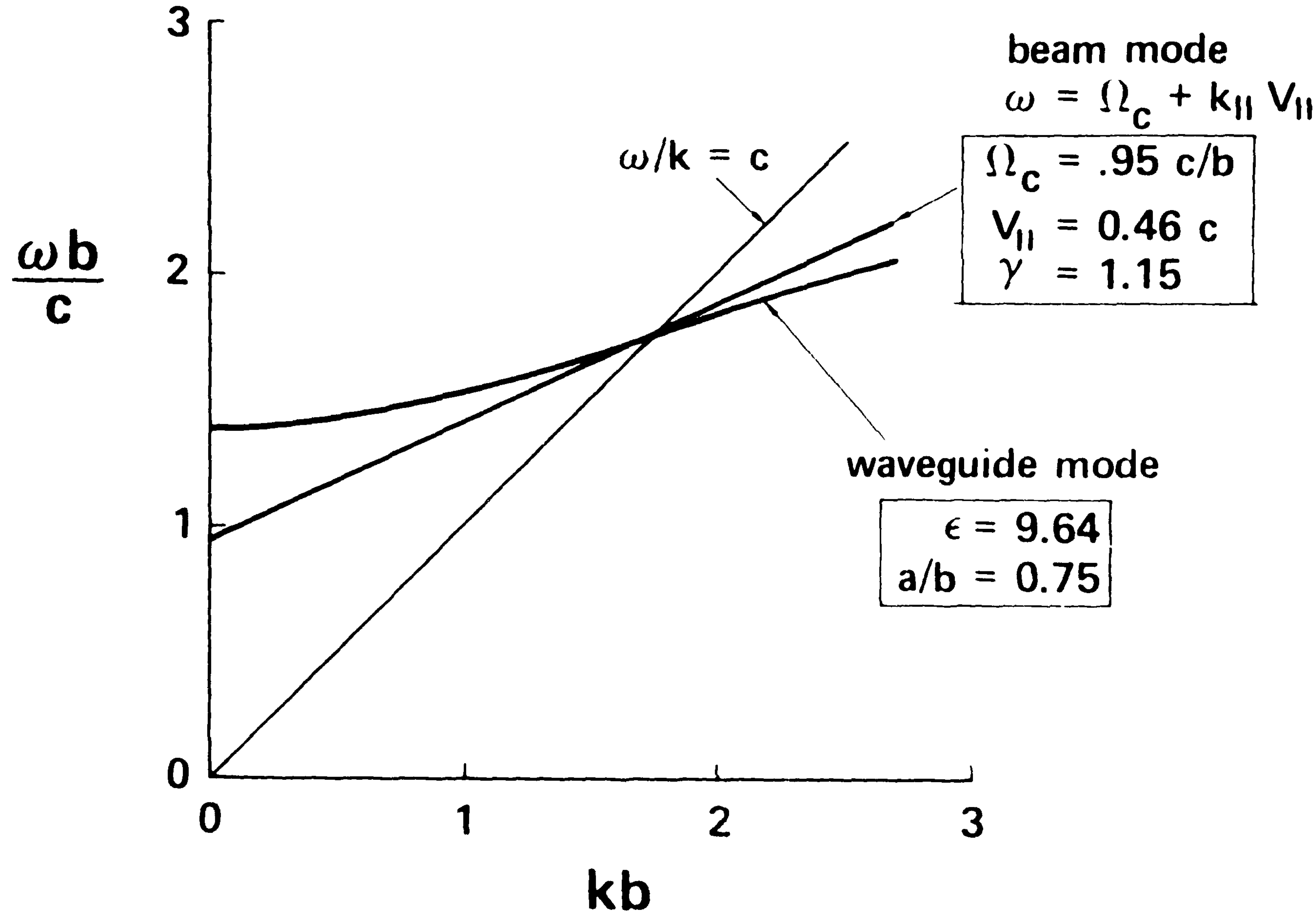

Figure 14 Dispersion diagram of cyclotron wave resonance line and slow wave mode for planned experiment.

8. Y. Carmel, K.R. Chu, M. Read, A.K. Ganguly, D. Dialetis, R. Seeley, J.S.Levine and V. L. Granatstein, Phys. Rev. Lett. 50, 112 (1983).

9. V.L. Bratman, N.C. Ginzburg, G.S. Nusinovich, M.I. Petelin and P.S. Strelkov, Int. J. Elec. 51, 541 (1981).

10. A.T. Lin, Int. J. Elec. 57, 1097 (1984).

11. I.E. Botvinnik, V.L. Bratman, A.B. Volkov, G.G.Denisov, B.D. Kolchugin and M.M. Ofitserov, Sov. Tech. Phys. Lett. 8, 596 (1982).

12. H. Crosby, J. Choe, Y. Song and A. Krall, Naval Surface Weapons Center Report 84-338 (1984).

II. Publications and Presentations

D.B. McDermott, N.C. Luhmann, Jr., A. Kupiszewski, and H.R. Jory, "Small-Signal Theory of a Large Electron Cyclotron Harmonic Maser," Phys. Fluids 26, 1936 (1983).

D.B. McDermott, N.C. Luhmann, Jr., D.S. Furuno, A. Kupiszewski, and H.R. Jory, "Operation of a Millimeter Wave Harmonic Gyrotron," Int. J. Infrared and MM Waves 4, 639 (1983).

D.B. McDermott, D.S. Furuno, N.C. Luhmann, Jr., "Enhancement of High Harmonic Gyrotron Gain by a Dielectric Rod," Int J. Infrared and MM Waves 4, 831 (1983).

D.B. McDermott, "Effect of Velocity Spread on Finite-Length Free Electron Laser Gain," Int. J. Infrared and MM Waves 4, 1015 (1983).

D.B. McDermott and N.C. Luhmann, Jr., "High-Harmonic Gyrotrons," Microwave Journal 27, 137 (1984).

D.B. McDermott, D.S. Furuno and N.C. Luhmann, Jr., "Production of Relativistic, Rotating Electron Beams by Gyro-Resonant RF-Acceleration in a TE_{111} Cavity," J. Appl. Physics 58, 4501 (1985).

D.B. McDermott, N.C. Luhmann, Jr., A Kupiszewski, D.S. Furuno, S.Y. Song, "Cyclotron Harmonic Maser for Far-Infrared Thomson Scattering Studies," 4th APS Topical Conf. on High Temperature Plasma Diagnostics, Boston, MA, August 1982.

F. Allen, Y. Bae, S.S.Iyer, C. Jou, A. Kupiszewski, N. Lee, N.C. Luhmann, Jr., D.B. McDermott, R.A.Metzer, D.S. Pan, W.A. Peebles, D. Rutledge, D. Umstadter, Y. Xu, and C.C. Yang, "Current Millimeter and Submillimeter Wave Source Development at UCLA, "USA-Japan Workshop on Submillimeter Diagnostic Techniques, Nagoya, Japan, Jan. 18-21, 1982.

D.B. McDermott, D.S. Furuno and N.C. Luhmann, Jr., "Millimeter-Wave Harmonic Gyrotron Results," IEEE Int. Conf. on Plasma Science, 1983.

D.B. McDermott, Haibo Cao and N.C. Luhmann, Jr., "A Cherenkov CARM," IEEE Int. Conf. on Plasma Science, 1987.

D.B. McDermott and N.C. Luhmann, Jr., "Operation of a Compact MM-Wave High-Harmonic Gyrotron," SPIE's 27th Annual Int. Technical Symposium 1983.

N.C. Luhmann, Jr., "UCLA Harmonic Gyrotron Program," seminar, Naval Research Laboratory, April 1983.

D.B. McDermott, D.S. Furuno, N.C. Luhmann, Jr., and P. Vitello, "Design and Operation of High-Harmonic Gyrotron Oscillators and Gyro-klystron Amplifiers," Technical Digest of 1983 International Electron Device Meeting, IEEE Cat. No. 83CH1973-7, 284 (1983).

D.B. McDermott, Haibo Cao, N.C. Luhmann, Jr., "A Cherenkov Cyclotron Autoresonance Maser," Technical Digest of 1985 Int. Electron Device Meeting (1985).

D.B. McDermott, D.S. Furuno, and N.C. Luhmann, Jr., "High- Harmonic Gyrotron Oscillators and Gyro-Klystron Amplifiers," IEEE MTT-S Int. Microwave Symposium Digest, IEEE Cat. No. 84CH2034-7, 359 (1984).

D.B. McDermott, "Harmonic Gyrotron Development at UCLA," Invited Seminar, Hughes Electron Device Division, Torrance, CA (March 1984).

N.C. Luhmann, Jr., "UCLA Harmonic Gyrotron Program," Invited Colloquim, Department of Physics, Tsinghua University, Taiwan (October, 1984).

D.B. McDermott, Haibo Cao and N.C. Luhmann, Jr., "A Cherenkov Cyclotron Autoresonance Maser," Fourth Int'l Symp. on Gyrotron and FEL, Chengdu, China (1986), to be publ. IEEE Trans. Plasma Science, special μ-wave issue.

D.B. McDermott, D.S. Furuno, N.C. Luhmann, Jr., W.J. Nunan, Haibo Cao, "Compact, High Power Millimeter Wave Sources," Sixth Int. Conf. High Power Particle Beams, Japan, 1986.

A. Kupiszewski, N.C. Luhmann, Jr. and H. Jory, "Compact Cyclotron Resonance Maser," Proc. Sixth Int. Conf. IR and mm-Waves, IEEE, #81CH1645-1MTT, W-2-5, 1981.

N.C. Luhmann, Jr., D.B. McDermott, D.S. Furuno, "Millimeter-Wave Harmonic Gyrotron Results," Proc. of 7th Int. Conf. on Infrared and Millimeter Waves, Marseilles, France, February 1983.

D.B. McDermott, N.C. Luhmann, Jr., S.Y. Song, "Theory of a Harmonic Gyrotron Using Axis-Encircling Electrons," to be published in Proc. of 7th Int. Conf. on Infrared and Millimeter Waves, Marseilles, France, February 1983.

D.B. McDermott, D.S. Furuno and N.C. Luhmann, Jr., "Enhancement of High Harmonic Gyrotron Gain by a Dielectric Rod," Proc. of Eighth Int. Conf. on Infrared and Millimeter Waves, IEEE Cat. No. 83CH1917-4, TH14 (1983).

D.B. McDermott, N.C. Luhmann, Jr. and D.S. Furuno (Invited Keynote Address), "Operation of a High-Harmonic Gyrotron," Proc. of Eighth Int. Conf. on Infrared and Millimeter Waves, IEEE Cat. No. 83CH1917-4, TH41 (1983).

D.B. McDermott and N.C. Luhmann, Jr., "A High Power, Fourth Harmonic Gyrotron," Proc. Ninth Int. Conf. Infrared and Millimeter Waves, 1984.

D.B. McDermott and N.C. Luhmann, Jr., "Suppression of Axial Mode Competion in a High Harmonic Gyromonotron," Proc. of the Tenth Int'l. Conf. on IR and mm-Waves, IEEE Cat. No. 85CH2204-6, Florida pg. 295 (1985).

D.B. McDermott, Haibo Cao and N.C. Luhmann, Jr., "A Cherenkov Cyclotron Autoresonance Maser," Proc. of the Eleventh Int'l Conf. on IR and mm-Waves, Italy, 1986

D.B. McDermott, N.C. Luhmann, Jr., A. Kupiszewski, D.S. Furuno, "Operation of a High Harmonic Compact Gyrotron," Bull. Am. Phys. 27, 1061 (1982).

N.C. Luhmann, Jr., D.B. McDermott, A. Kupiszewski, S.Y. Song, H.R. Jory, "Small-Sig Theory of a Large Orbit Electron Cyclotron Harmonic Maser," Bull. Am. Phys. 27, 1061 (1982).

G. Carandang, D.B. McDermott, N.C. Luhmann, Jr., D.S. Furuno, "Operation of a High Harmonic Gyrotron," Bull. Am. Phys. 28, 1058 (1983).

D.B. McDermott, D.S. Furuno, N.C. Luhmann, Jr., "Enhancement of High-Harmonic Gyrotron Gain by a Dielectric Rod," Bull. Am. Phys. 28, 1192 (1983).

B. Chang, D.B. McDermott, N.C. Luhmann, Jr., "A High Power, Fourth Harmonic Gyrotron Experiment," Bull. Am. Physical Soc. 29, 1180 (1984).

D.B. McDermott and N.C. Luhmann, Jr., "Suppression of Axial Mode Competition in High Harmonic Gyromonotrons," Bull. Am. Physical Soc. 30, 1509 (1985).

N.C. Luhmann, Jr., "High Harmonic Millimeter Wave, Large Orbit Gyrotron Oscillators and Amplifiers," Invited Talk, Bull. Am. Phys. Soc. 30, 1618 (1985).

D.B. McDermott and N.C. Luhmann, Jr., "A Complex High Harmonic Gyrotron," Bull. Am. Physical Soc. 31, 1386 (1986).

Haibo Cao, D.B. McDermott and N.C. Luhmann, Jr., "A Cherenkov Cyclotron Autoresonance Maser," Bull. Am. Physical Soc. 31, 1505 (1986).

H.B. Cao, K.Z. Cheng, K.R. Chu, D.S. Furuno, T.H. Kho, C.S. Kou, A.T. Lin, N.C

Luhmann, Jr., D.B. McDermott, P. Vitello, "Fast Wave Device Research at UCLA," High Power mm Wave Fast Devices Workshop, NRL, Washington, D.C., 1987.